

Suitably impressive thesis title

Robin Timmis

Your College
University of Oxford

*A thesis submitted for the degree of
Doctor of Philosophy*

Michaelmas 2014

Abstract

Your abstract text goes here. Check your departmental regulations, but generally this should be less than 300 words. See the beginning of Chapter ?? for more.

Lorem ipsum dolor sit amet, consectetur adipiscing elit. Pellentesque sit amet nibh volutpat, scelerisque nibh a, vehicula neque. Integer placerat nulla massa, et vestibulum velit dignissim id. Ut eget nisi elementum, consectetur nibh in, condimentum velit. Quisque sodales dui ut tempus mattis. Duis malesuada arcu at ligula egestas egestas. Phasellus interdum odio at sapien fringilla scelerisque. Mauris sagittis eleifend sapien, sit amet laoreet felis mollis quis. Pellentesque dui ante, finibus eget blandit sit amet, tincidunt eu neque. Vivamus rutrum dapibus ligula, ut imperdiet lectus tincidunt ac. Pellentesque ac lorem sed diam egestas lobortis.

Suspendisse leo purus, efficitur mattis urna a, maximus molestie nisl. Aenean porta semper tortor a vestibulum. Suspendisse viverra facilisis lorem, non pretium erat lacinia a. Vestibulum tempus, quam vitae placerat porta, magna risus euismod purus, in viverra lorem dui at metus. Sed ac sollicitudin nunc. In maximus ipsum nunc, placerat maximus tortor gravida varius. Suspendisse pretium, lorem at porttitor rhoncus, nulla urna condimentum tortor, sed suscipit nisi metus ac risus.

Aenean sit amet enim quis lorem tristique commodo vitae ut lorem. Duis vel tincidunt lacus. Sed massa velit, lacinia sed posuere vitae, malesuada vel ante. Praesent a rhoncus leo. Etiam sed rutrum enim. Pellentesque lobortis elementum augue, at suscipit justo malesuada at. Lorem ipsum dolor sit amet, consectetur adipiscing elit. Praesent rhoncus convallis ex. Etiam commodo nunc ex, non consequat diam consectetur ut. Pellentesque vitae est nec enim interdum dapibus. Donec dapibus purus ipsum, eget tincidunt ex gravida eget. Donec luctus nisi eu fringilla mollis. Donec eget lobortis diam.

Suspendisse finibus placerat dolor. Etiam ornare elementum ex ut vehicula. Donec accumsan mattis erat. Quisque cursus fringilla diam, eget placerat neque bibendum eu. Ut faucibus dui vitae dolor porta, at elementum ipsum semper. Sed ultrices dui non arcu pellentesque placerat. Etiam posuere malesuada turpis, nec malesuada tellus malesuada.

Suitably impressive thesis title



Robin Timmis
Your College
University of Oxford

A thesis submitted for the degree of
Doctor of Philosophy

Michaelmas 2014

Acknowledgements

Personal

This is where you thank your advisor, colleagues, and family and friends.

 Lorem ipsum dolor sit amet, consectetur adipiscing elit. Vestibulum feugiat et est at accumsan. Praesent sed elit mattis, congue mi sed, porta ipsum. In non ullamcorper lacinia. Quisque volutpat tempus ligula ac ultricies. Nam sed erat feugiat, elementum dolor sed, elementum neque. Aliquam eu iaculis est, a sollicitudin augue. Cras id lorem vel purus posuere tempor. Proin tincidunt, sapien non dictum aliquam, ex odio ornare mauris, ultrices viverra nisi magna in lacinia. Fusce aliquet molestie massa, ut fringilla purus rutrum consectetur. Nam non nunc tincidunt, rutrum dui sit amet, ornare nunc. Donec cursus tortor vel odio molestie dignissim. Vivamus id mi erat. Duis porttitor diam tempor rutrum porttitor. Lorem ipsum dolor sit amet, consectetur adipiscing elit. Sed condimentum venenatis consectetur. Lorem ipsum dolor sit amet, consectetur adipiscing elit.

 Aenean sit amet lectus nec tellus viverra ultrices vitae commodo nunc. Mauris at maximus arcu. Aliquam varius congue orci et ultrices. In non ipsum vel est scelerisque efficitur in at augue. Nullam rhoncus orci velit. Duis ultricies accumsan feugiat. Etiam consectetur ornare velit et eleifend.

 Suspendisse sed enim lacinia, pharetra neque ac, ultricies urna. Phasellus sit amet cursus purus. Quisque non odio libero. Etiam iaculis odio a ex volutpat, eget pulvinar augue mollis. Mauris nibh lorem, mollis quis semper quis, consequat nec metus. Etiam dolor mi, cursus a ipsum aliquam, eleifend venenatis ipsum. Maecenas tempus, nibh eget scelerisque feugiat, leo nibh lobortis diam, id laoreet purus dolor eu mauris. Pellentesque habitant morbi tristique senectus et netus et malesuada fames ac turpis egestas. Nulla eget tortor eu arcu sagittis euismod fermentum id neque. In sit amet justo ligula. Donec rutrum ex a aliquet egestas.

Institutional

If you want to separate out your thanks for funding and institutional support, I don't think there's any rule against it. Of course, you could also just remove the subsections and do one big traditional acknowledgement section.

 Lorem ipsum dolor sit amet, consectetur adipiscing elit. Ut luctus tempor ex at pretium. Sed varius, mauris at dapibus lobortis, elit purus tempor neque,

facilisis sollicitudin felis nunc a urna. Morbi mattis ante non augue blandit pulvinar. Quisque nec euismod mauris. Nulla et tellus eu nibh auctor malesuada quis imperdiet quam. Sed eget tincidunt velit. Cras molestie sem ipsum, at faucibus quam mattis vel. Quisque vel placerat orci, id tempor urna. Vivamus mollis, neque in aliquam consequat, dui sem volutpat lorem, sit amet tempor ipsum felis eget ante. Integer lacinia nulla vitae felis vulputate, at tincidunt ligula maximus. Aenean venenatis dolor ante, euismod ultrices nibh mollis ac. Ut malesuada aliquam urna, ac interdum magna malesuada posuere.

Abstract

Your abstract text goes here. Check your departmental regulations, but generally this should be less than 300 words. See the beginning of Chapter ?? for more.

 Lorem ipsum dolor sit amet, consectetur adipiscing elit. Pellentesque sit amet nibh volutpat, scelerisque nibh a, vehicula neque. Integer placerat nulla massa, et vestibulum velit dignissim id. Ut eget nisi elementum, consectetur nibh in, condimentum velit. Quisque sodales dui ut tempus mattis. Duis malesuada arcu at ligula egestas egestas. Phasellus interdum odio at sapien fringilla scelerisque. Mauris sagittis eleifend sapien, sit amet laoreet felis mollis quis. Pellentesque dui ante, finibus eget blandit sit amet, tincidunt eu neque. Vivamus rutrum dapibus ligula, ut imperdiet lectus tincidunt ac. Pellentesque ac lorem sed diam egestas lobortis.

 Suspendisse leo purus, efficitur mattis urna a, maximus molestie nisl. Aenean porta semper tortor a vestibulum. Suspendisse viverra facilisis lorem, non pretium erat lacinia a. Vestibulum tempus, quam vitae placerat porta, magna risus euismod purus, in viverra lorem dui at metus. Sed ac sollicitudin nunc. In maximus ipsum nunc, placerat maximus tortor gravida varius. Suspendisse pretium, lorem at porttitor rhoncus, nulla urna condimentum tortor, sed suscipit nisi metus ac risus.

 Aenean sit amet enim quis lorem tristique commodo vitae ut lorem. Duis vel tincidunt lacus. Sed massa velit, lacinia sed posuere vitae, malesuada vel ante. Praesent a rhoncus leo. Etiam sed rutrum enim. Pellentesque lobortis elementum augue, at suscipit justo malesuada at. Lorem ipsum dolor sit amet, consectetur adipiscing elit. Praesent rhoncus convallis ex. Etiam commodo nunc ex, non consequat diam consectetur ut. Pellentesque vitae est nec enim interdum dapibus. Donec dapibus purus ipsum, eget tincidunt ex gravida eget. Donec luctus nisi eu fringilla mollis. Donec eget lobortis diam.

 Suspendisse finibus placerat dolor. Etiam ornare elementum ex ut vehicula. Donec accumsan mattis erat. Quisque cursus fringilla diam, eget placerat neque bibendum eu. Ut faucibus dui vitae dolor porta, at elementum ipsum semper. Sed ultrices dui non arcu pellentesque placerat. Etiam posuere malesuada turpis, nec malesuada tellus malesuada.

Contents

List of Figures	ix
A List of Symbols and Abbreviations	xi
1 Introduction	1
1.1 A plan	1
1.2 The definition of a plasma	2
1.2.1 The Debye length	3
1.2.2 The plasma parameter	4
1.2.3 Collisionality and the plasma frequency	4
1.3 The Lawson-Woodward theorem	6
2 The Zero Vector Potential Absorption Mechanism	7
2.1 Introduction	7
2.1.1 ZVP electron bunch energies	15
2.1.2 ZVP bunches oblique incidence scaling and internal bunch structure	18
2.2 Defining characteristics of the ZVP mechanism	23
2.3 Numerical simulations of the ZVP mechanism	24
2.3.1 The ZVP mechanism in 3D	24
2.3.2 The ZVP electron bunch	26
2.3.3 Total electron bunch energy scaling	34
3 Miscellaneous notes	37
3.1 ORION experiment	37
3.1.1 Frames of reference	37
3.1.2 ORION interaction geometry	41
3.1.3 Condition on validity of hole boring expression	42
Appendices	
A General plasma physics	47
A.1 Geometric transverse emittance	47
References	51

List of Figures

1.1	Diagram to illustrate the plasma frequency derivation. THIS FIGURE NEEDS E POINTING THE OTHER WAY	5
2.1	Diagram of a p -polarised laser pulse incident on an ablating overdense plasma.	11
2.2	Simulation results from a 3D PIC! (PIC!) simulation of the Zero Vector Potential (ZVP) mechanism.	25
2.3	Comparison between the initial 3D simulation and a lower resolution version.	27
2.4	2D PIC simulation results qualitatively describing typical mass- limited ZVP electron bunch structure.	29
2.5	Mean mass-limited ZVP electron bunch normalised kinetic energies extracted from 2D PIC simulations.	31
2.6	The relative errors for each mean energy data point compared to figure 2.5.	34
3.1	38
3.2	ORION target chamber geometry showing the location of the target (TCC) and OHREX spectrometer and the green (SP1) and infra-red (SP2) beamlines and their corresponding polarisations.	41

x

A List of Symbols and Abbreviations

e	Absolute charge of an electron = 1.602×10^{-19} C
ϵ_0	Permittivity of free space = 8.854×10^{-12} F m $^{-1}$
λ_D	Debye length $\equiv \sqrt{\frac{\epsilon_0 K T_e}{n_e e^2}}$
n_e	Plasma electron number density as a function of position
n_i	Plasma ion number density as a function of position
T_e	Plasma electron temperature
Z	Ion charge state in units of e
1D, 2D, 3D	One-, two- or three-dimension(al)
Otter	One of the finest of water mammals.
Hedgehog	Quite a nice prickly friend.

xii

Neque porro quisquam est qui dolorem ipsum quia dolor sit amet, consectetur, adipisci velit...

There is no one who loves pain itself, who seeks after it and wants to have it, simply because it is pain...

— Cicero's *de Finibus Bonorum et Malorum*

1

Introduction

Contents

1.1	A plan	1
1.2	The definition of a plasma	2
1.2.1	The Debye length	3
1.2.2	The plasma parameter	4
1.2.3	Collisionality and the plasma frequency	4
1.3	The Lawson-Woodward theorem	6

1.1 A plan

Actually the very first thing to say will be the stuff about light i think, about diagnostic tools essentially always being about controlling the various properties of light (ie electromagnetic waves)

sections to include start with the laser and our entrance into the multi-petawatt regime with no signs of stopping - ref 40 in alex savin thesis - it looks like that is saying huge growth in laser power check that and maybe write in thesis but don't include the figure. Also include description of CPA and OPCPA what is a plasma modelling plasma with PIC codes intense lasers and absorption mechanisms?? yes for sure but dont do all just those just below ZVP simulation units and similarity parameter Frames of reference - lab, sim, ablating front sruface of plasma

what is the story? Based on first section by Alex after the abstract Plasma is ubiquitous in our known universe and plasma provides us huge opportunities as a tool to improve our lives (From chen) what we can see in the sky is a result of that stuff being in the plasma state. Lasers can do so much now and are only getting more powerful all the time thanks to CPA and since developments (discuss) Simultaneously our ability to understand the physics has been aided by an explosion in computing power (peter HEDP paper) In this thesis we discuss some of the opportunities that relativistic laser plasma physics offers us with solid density targets - note that note about solids v gases at this point. Perhaps even before the debye length, define what we mean by the temperature of the plasma??

An unused statement about ion immobility Assume for now that the ion-electron mass ratio is infinite, that is to say the ions are approximately immobile for the timescales under consideration, generally true for a fair few relativistic laser pulse cycles (In later sections the mobility of plasma ions will prove very important but for now this is ignored.).

1.2 The definition of a plasma

As outlined in F. Chen's definitive textbook 'Introduction to Plasma Physics and Controlled Fusion' [[chen20116](#)], a plasma must fulfil three criteria, namely,

1. Ionisation: a plasma must consist of both charged and neutral particles, of course this alone cannot define a plasma, any gas will contain some degree of ionisation;
2. Quasineutrality: while locally there can be (often extreme) electromagnetic forces and charge concentrations at work, over the length scales of the plasma, such forces are screened out and the plasma bulk remains net neutral in charge;
3. Collective behaviour: unlike in a gas where collisions dominate, the particles in a plasma generate electromagnetic fields that interact at a distance and

thus a particle's motion depends not only on its immediate viscosity but on the surrounding plasma conditions, indeed often it is the so-called 'collisionless' plasmas where collisions can be safely neglected that are of most interest, as is the focus of this thesis.

1.2.1 The Debye length

The Debye length describes the extent to which a plasma can shield electromagnetic fields within and so remain quasineutral. Consider an infinitely extending plasma with a test charge placed at some point, then what would be the potential $\phi(\mathbf{x})$? If the plasma had no kinetic energy, the charged particles would arrange themselves immediately adjacent to the test charge and once this equilibrium state was reached there would be no electromagnetic fields present. Realistically the plasma will have some temperature, likely a very large temperature and so some particles will be able to escape the potential of the test charge and thus leak electromagnetic fields into the plasma bulk. Poisson's equation reads

$$\epsilon_0 \nabla^2 \phi = -e(Zn_i - n_e), \quad (1.1)$$

where $\epsilon_0 = 8.854 \times 10^{-12} \text{ F m}^{-1}$ is the permittivity of free space, $e = 1.602 \times 10^{-19} \text{ C}$ is the charge of an electron, Z is the plasma ion charge in units of e and n_i and n_e are the number densities of plasma ions and electrons.

Since the electrons are significantly more mobile than the ions due to their lower mass, it is in general the electrons and not the ions that respond to the test charge and the ions can be assumed to provide a constant background of positive charge density. If the number density of electrons follows a Boltzmann temperature distribution in the presence of a potential energy $-e\phi$, then

$$n_e = n_{e,0} e^{e\phi/KT_e}, \quad (1.2)$$

where $n_{e,0}$ is the electron number density far from the test charge, $n_i = n_{e,0}/Z$ and KT_e is the electron temperature. Note that in plasmas it is very common for different species to have differing temperatures depending on the mechanism for energy absorption and the timescales for collisions compared to the timescale of the study.

Substituting equation 1.2 into equation 1.1 and Taylor expanding the exponential term in the limit that the plasma is weakly coupled ($e\phi \ll KT_e$), obtains

$$\nabla^2\phi = \frac{\phi}{\lambda_D^2}, \quad (1.3)$$

where

$$\lambda_D \equiv \sqrt{\frac{\epsilon_0 K T_e}{n_e e^2}}, \quad (1.4)$$

is the *Debye length* and describes the thickness of the charge sheath surrounding the test charge. For quasineutrality to hold for the plasma bulk, its spatial dimensions must extend beyond a few Debye lengths.

1.2.2 The plasma parameter

In order for the above description to be statistically valid, there must be a large number of charged particles within the shielding sheath. The number of particles within the Debye sphere can be computed as

$$N_D = \frac{4}{3}\pi\lambda_D^3 n. \quad (1.5)$$

Note that, as discussed above, in most cases it is most suitable to choose the number density n to be the number density of electrons. To ensure the plasma is suitably ionised (criterion 1) and that the plasma engages in collective behaviour (criterion 3),

$$N_D \ggg 1. \quad (1.6)$$

1.2.3 Collisionality and the plasma frequency

Collective behaviour not only depends on the ability for large numbers of particles to interact via electromagnetic forces but that these forces dominate over collisions in describing particle trajectories. Taking ω as the typical frequency of plasma oscillations and τ as the average time between collisions, for a plasma (as opposed to a gas) must satisfy

$$\omega\tau > 1. \quad (1.7)$$

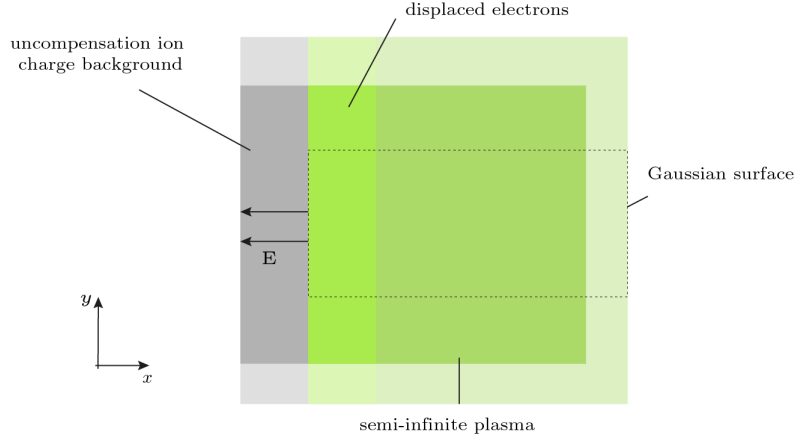


Figure 1.1: Diagram to illustrate the plasma frequency derivation. THIS FIGURE NEEDS E POINTING THE OTHER WAY

It now remains to determine what is the typical frequency of collisions in a given plasma. While the types of plasma waves and their associated frequencies of oscillation are multitudinous, the characteristic frequency, the *plasma frequency*, ω_p , is the most straightforward. It describes the response of electrons to charge imbalances within an infinite uniform plasma at rest in the absence of magnetic fields or temperature fluctuations. As noted in section 1.2.1, the ions provide a constant background of positive charge.

Consider a semi-infinite plasma existing for $x > 0$, with electron density n_e and ion density n_e/Z of charge state Z^1 . Suppose the electron fluid is displaced by some perfectly isotropic force into the plasma bulk a distance $(\Delta x)\hat{\mathbf{x}}$ as in figure 1.1. The total charge of displaced electrons within a surface area of σ is

$$Q = -en_e\sigma\Delta x. \quad (1.8)$$

Applying Gauss' law to the surface detailed in figure 1.1, the uncompensated charge leads to

$$-\sigma E\hat{\mathbf{x}} = \frac{Q}{\epsilon_0}\hat{\mathbf{x}} = -\frac{en_e\sigma\Delta x}{\epsilon_0}\hat{\mathbf{x}} \quad (1.9)$$

at the electron surface. By the Lorentz force, the displaced electrons will experience a restoring force, $-eE\hat{\mathbf{x}}$, perpendicular to the surface due to the electron-ion charge

¹This description has direct relevance to the Zero Vector Potential mechanism which will be made clear later.

imbalance. The equation of motion for electrons on that surface is therefore

$$m_e \frac{d^2 \Delta x}{dt^2} = -eE = -\frac{e^2 n_e}{\epsilon_0} \Delta x. \quad (1.10)$$

Equation 1.10 clearly describes a simple harmonic oscillator with a characteristic frequency given by the plasma frequency,

$$\omega_p = \sqrt{\frac{e^2 n_e}{m_e \epsilon_0}}. \quad (1.11)$$

1.3 The Lawson-Woodward theorem

The Lawson-Woodward theorem states that there can be no net electron energy gain using laser fields [esarey_2009_PhysicsLaserdrivenPlasmabaseda], quite at odds with one of the primary aims of this thesis, that is, the acceleration of electrons. There are, however, several conditions that must be met, namely,

1. The interaction region is infinite;
2. The interaction occurs in a vacuum;
3. The electron is ultra-relativistic ($v \approx c$) along the acceleration gradient;
4. No electro- or magnetostatic fields are present;
5. Non-linear effects are neglected.

Several of these will be applicable to the various accelerations of electrons considered. It is this final condition that is most damning, throughout this thesis the ultra-relativistic laser pulses under consideration ensure non-linear effects cannot be neglected. It is indeed such non-linearities that are of interest.

2

The Zero Vector Potential Absorption Mechanism

Contents

2.1	Introduction	7
2.1.1	ZVP electron bunch energies	15
2.1.2	ZVP bunches oblique incidence scaling and internal bunch structure	18
2.2	Defining characteristics of the ZVP mechanism	23
2.3	Numerical simulations of the ZVP mechanism	24
2.3.1	The ZVP mechanism in 3D	24
2.3.2	The ZVP electron bunch	26
2.3.3	Total electron bunch energy scaling	34

2.1 Introduction

Of primary interest in this thesis is the interaction of a relativistically intense short pulse laser interacting with a solid density plasma target with a sharp density gradient. Now is presented the Zero Vector Potential mechanism of attosecond absorption of laser pulse energy, proposed by *Baeva et al* [**baevaTheoryHighorderHarmonic2006**] and later developed by *Savin et al* [**savinAttosecondscaleAbsorptionExtreme2017**, **savinEnergyAbsorptionLaserQED2019**]. Laser energy absorption in dense plasmas was first proposed by Wilks and Kruer [**wilksAbsorptionUltraIntenseLaser1992**],

a ponderomotive mechanism where plasma electrons are heated directly by the laser pulse via the so-called $\mathbf{J} \times \mathbf{B}$ force.

This thesis focuses on the so-called ‘post-ponderomotive’ regime where the frequency of the plasma oscillations ($\omega_p \sim \sqrt{n_e}$) are greater than the $\mathbf{J} \times \mathbf{B}$ induced plasma electron oscillations at $2\omega_L$. The plasma electrons are then fast enough to compensate the ponderomotive pressure of the laser pulse with the formation of electrostatic fields between electrons and ions and so respond adiabatically to the $\mathbf{J} \times \mathbf{B}$ force. Hence plasma electrons cannot be heated directly by the laser pulse. Note that this requires a sufficiently steep density gradient around the relativistic critical density surface (where $S = 1$) to shift the main interaction to a region where this condition on the overdensity is satisfied. In this case the ponderomotive pressure of the laser compresses the electrons at the front surface of the plasma and so shifts the laser-plasma surface interaction to plasma densities well beyond the relativistic critical density, leaving behind a positive space charge. This electron-ion charge separation leads to the formation of a *pseudo-capacitor* electrostatic field.

Interestingly working through the condition between ω_p and ω_L in normalised units suggests the criterion for this regime is $S > 4$, slightly more constraining than $S > 1$ as is typically stated [**savinModellingLaserPlasmaInteractions2019**].

[Come back to this and write up stuff about actually it being the relativistic frequency and critical density surfaces that matter and how this does indeed put a stricter condition on the bulk S value]

So we have entered a regime of adiabaticity where the plasma skin layer is confined within a potential well consisting of the ponderomotive pressure and the Coulomb potential. Consider a relativistic linearly polarised laser pulse obliquely incident, with an angle of incidence of θ , on a semi-infinite plasma, existing for $x > 0$. The Hamiltonian of a single electron confined within the potential well [**goldsteinClassicalMechanics2013**] is

$$\mathcal{H} = c\sqrt{m_e^2c^2 + |\mathbf{p}|^2} - e\Phi. \quad (2.1)$$

Here the first term is the electron energy, U , extracted from the invariant of the relativistic 4-momentum of the electron, $\mathbf{P}^\mu = (U/c, \mathbf{p})$,

$$\mathbf{P}^\mu \cdot \mathbf{P}_\mu = \frac{U^2}{c^2} - |\mathbf{p}|^2 = m^2 c^2. \quad (2.2)$$

Note that while there has been growing interest in the curvature of spacetime by relativistic lasers [cite edward here], for modern high power lasers this effect is small and not relevant for this thesis. Throughout the inner product of 4-vectors is defined with the Minkowski Metric. [find alex citation on pg 89 of thesis]

The second term of equation 2.1 describes the contribution to the electron's energy from the electrostatic potential of the pseudo-capacitor. Decomposing the electron's 3-momentum into orthogonal components: p_{prop} , along the laser propagation direction, p_{pol} , along the polarisation axis of the laser pulse and p_\perp , perpendicular to both, two simplifications can be made. Firstly, by canonical conservation of transverse momentum, $p_{\text{pol}} = eA$, where A is the laser vector potential. Secondly, in the case of a p -polarised laser pulse (the known optimum for ZVP electron bunch generation), the forces at play confine the electron trajectory to the $p_{\text{prop}}-p_{\text{pol}}$ plane and the interaction geometry is in essence two-dimensions (2D).

[include a diagram alluding to this?-it is basically since B is out of the plane and all other E fields are in the plane, also perhaps provide a foot note here to explain how incidentally this all provides a succinct explanation of why p is better?]

Explicitly, the Hamiltonian is now

$$\mathcal{H} = c\sqrt{m_e^2 c^2 + p_{\text{prop}}^2 + e^2 A^2} - e\Phi. \quad (2.3)$$

From equation 2.3 it is clear that should the vector potential pass through zero, one of the walls of the potential well is suppressed, allowing electrons in the skin layer to escape the plasma, breaking adiabaticity. The necessity of vector potential zeros for this violent reconstruction of the plasma surface led Baeva et al [**baevaZeroVectorPotential2011**] to coin the term ‘Zero Vector Potential’ mechanism to describe this process. Indeed, while in standard calculations a laser pulse will exponentially decay within a skin layer without passing through zero,

Baeva et al [**baevaZeroVectorPotential2011**] were able to demonstrate in **PIC!** simulations that for this regime, zeros are able to propagate through the skin layer of the plasma. The explanation for this difference in mechanics relies on a Doppler shift in the laser field due to the relativistic motion of the ablating plasma surface, and the mathematical formalism of this process proceeds as follows.

[I think before this point it would be good to enter in the language of electron bunches or sheaths - I will continue the dicussion assuming this concept has been introduced].

As the ZVP mechanism is a relativistic phenomenon, it is essential to consider the laser pulse propagating through a relativistically ablating electron bunch (i.e. with some component of its velocity anti-parallel to the laser pulse propagation direction). Transforming to the rest frame of the ablating front, beyond the relativistic critical density surface, the vector potential of the laser pulse will be an evanescent wave, at the spatial centre of the laser pulse, it can be described simply by

$$\mathbf{A}'_{\text{L}}(t', r') = A'_0 \cos(\omega'_{\text{L}} t') \exp(-r'/\delta') \hat{\mathbf{r}}'_{\text{pol}} = A'_0 \hat{\mathbf{r}}'_{\text{pol}}, \quad (2.4)$$

where the primed symbols indicate that these quantities are measured in the rest frame of the expanding front, A'_0 is the vector potential amplitude and ω'_{L} is the frequency of the laser pulse, r' is the propagation distance of the laser into the plasma, δ' is the skin depth and $\hat{\mathbf{r}}'_{\text{pol}}$ a unit vector defining the polarisation direction of the laser pulse. Un-primed coordinates will indicate the lab frame measurements.

[For sure include a diagram of this]

While in previous demonstrations of the vector potential zeros, it was assumed that the ablation occurs normal to plasma surface, it is now known that this ablation occurs in the specular reflection direction and it is necessary to confirm that zeros are still predicted. Consider a p-polarised laser pulse confined to the x - y plane incident with an angle of incidence θ on an ablating overdense plasma expanding with velocity $-v_f \hat{\mathbf{x}}$ in the lab frame, as in figure 2.1. The direction of polarisation is

$$\hat{\mathbf{r}}_{\text{pol}} = \hat{\mathbf{x}} \sin 2\theta - \hat{\mathbf{y}} \cos 2\theta \quad (2.5)$$

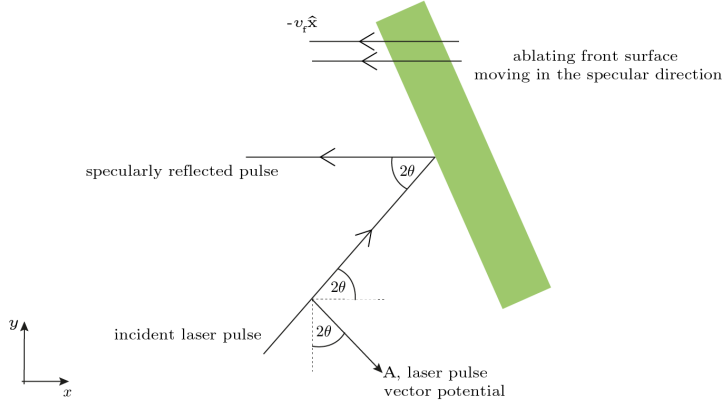


Figure 2.1: Diagram of a p -polarised laser pulse incident on an ablating overdense plasma. The laser is incident obliquely at an angle of θ and is reflected specularly. The plasma ablates specularly also. The interaction geometry is confined to a 2D plane.

and the velocity of the rest frame of the ablating front relative to the lab frame is $-v_f \hat{x}$.

Applying the Lorentz transformation to the electromagnetic 4-potential,

$$\mathbf{A}_\mu = (\phi/c, \mathbf{A}), \quad (2.6)$$

explicitly,

$$\mathbf{A}'_\mu = \Lambda_\nu^\mu \mathbf{A}_\nu, \quad (2.7)$$

where Λ_ν^μ , the Lorentz transform in this geometry is

$$\Lambda_\nu^\mu = \begin{pmatrix} \gamma & -\beta\gamma & 0 & 0 \\ -\beta\gamma & \gamma & 0 & 0 \\ 0 & 0 & 1 & 0 \\ 0 & 0 & 0 & 1 \end{pmatrix} \quad (2.8)$$

and here $\beta = -v_f/c$, $\gamma = 1/\sqrt{1-\beta^2}$. Immediately from the y -coordinate transformation,

$$A'_L \cos 2\theta' = A_L \cos 2\theta. \quad (2.9)$$

Applying the headlight effect for a source moving at an angle 2θ to the boosted frame,

$$\cos(2\theta') = \frac{\cos(2\theta) - \beta}{1 - \beta \cos(2\theta)} \quad (2.10)$$

and rearranging equation 2.9, the vector potential in the lab frame is

$$A_L = \frac{1 - \beta \sec(2\theta)}{1 - \beta \cos(2\theta)} A'_0 \cos(\omega'_L t') \exp(-r'/\delta'). \quad (2.11)$$

Writing the boosted frame space-time coordinates in terms of the lab frame coordinates,

$$ct' = \gamma(ct - \beta x), \quad (2.12)$$

$$x' = \gamma(x - \beta ct), \quad (2.13)$$

yields

$$A_L = A_0 \cos(\omega_L t - kx) \exp\left(-\frac{\sqrt{(x - \beta ct)^2 + (y/\gamma)^2}}{\delta}\right), \quad (2.14)$$

where

$$A_0 = \frac{1 - \beta \sec(2\theta)}{1 - \beta \cos(2\theta)} A'_0, \quad (2.15)$$

$$\omega_L = \gamma \omega'_L, \quad (2.16)$$

$$k = \frac{\beta \gamma \omega'_L}{c}, \quad (2.17)$$

$$\delta = \frac{\delta'}{\gamma}. \quad (2.18)$$

The oscillatory term in equation 2.14 demonstrates the propagation of vector potential zeros within the plasma target. From the structure of this term it would appear that these zeros are expelled from the plasma along the specular direction at a speed (recall beta is negative - change this earlier in the theory so that that negative sign is more explicit in the result.)

$$v_\phi = \frac{\omega_L}{k} = \frac{c}{\beta} = -\frac{c^2}{v_f}. \quad (2.19)$$

Could also discuss here about how relativistic similarity theory derives that zeros move at speed c but how that cannot be valid since then we would always have infinitely thin radiation pulses, unless there is an extended range of zero? I suppose there is some radiation happening around the peak? Good questions.. One remaining consideration is we require that the zero gets through the whole electron bunch which is generally at very high density but is also very thin, in a way is this skin depth

not what precisely determines the bunch width? The bunch will be compressed until the skin depth goes to zero across it perhaps? Things to think about.

Qualitatively, and in summary, for sufficiently intense laser pulses, electrons on the radiated surface of a solid target are accelerated by the laser to relativistic velocities at a fraction of a laser pulse cycle and therefore electrons both follow similar trajectories and are able to respond adiabatically to the $\mathbf{J} \times \mathbf{B}$ force of the laser pulse. They therefore form a high charge density thin coherent electron sheath on the front surface of the plasma but displaced inwards from the immobile ions (ions are approximately immobile on the timescale of a laser pulse cycle) via the ponderomotive pressure of the laser. This charge separation generates a longitudinal electrostatic pseudocapacitor field that confines electrons to a potential well on the front surface of the plasma, preventing further propagation of the electron bunch into the plasma bulk. When the zero of the vector potential passes through the electron bunch, the ponderomotive pressure instantaneously vanishes and electrons are ejected specularly from the target, copropagating with the zeroes and gaining energy as they discharge the pseudocapacitor field. Coherent synchrotron emission occurs concurrently. The electron bunch is then rotated by the laser pulse and launched into the bulk at high energy.

Something to think about: which comes first? electron bunch acceleration across pseudo capacitor or zeros? Laser accelerates electrons in laser propagation direction, however cannot propagate further into the plasma so only get motion parallel to surface, once potential well disrupted, acceleration is perpendicular to surface so combined, electrons travel in specular direction. So actually what we are saying is the zeros will go in whatever direction the surface ablates in, but the surface will move in a direction dependent on the components of electron

The headlight effect

This most likely goes in the appendix. But storing here for now.

The headlight effect describes the beaming of an isotropically emitting source travelling at some velocity relative to an observer. Consider the geometry of figure

2.1 with the source (the laser pulse) travelling at an angle 2θ to the observer (in this case, the ablating front). A photon with energy E emitted from the rest frame of the source (in this case the lab frame) has a 4-momentum

$$\mathbf{P}_\mu = \left(\frac{E}{c}, \frac{E}{c} \cos 2\theta, \frac{E}{c} \sin 2\theta \right). \quad (2.20)$$

As the interaction geometry is confined to a 2D plane, the z -component can be safely neglected. Applying the lorentz boost of equation 2.8,

$$\begin{aligned} \frac{E'}{c} &= \gamma \left(\frac{E}{c} - \beta \frac{E}{c} \cos 2\theta \right) \\ \frac{E'}{c} \cos 2\theta' &= \gamma \left(\frac{E}{c} \cos 2\theta - \beta \frac{E}{c} \right). \end{aligned} \quad (2.21)$$

Solving these equations for the angle in the boosted frame,

$$\cos 2\theta' = \frac{\cos 2\theta - \beta}{1 - \beta \cos 2\theta}. \quad (2.22)$$

Conservation of generalised transverse momentum

This should most likely go in the appendix/ before ZVP Hamiltonian discussion.

Whilst it is commonly stated within the field of laser-solid interactions, it would appear that some nuance/detail is missing from the discussion which in turn shrouds the ZVP mechanism in confusion.

Consider a holonomic system of N relativistic particles under the influence of electromagnetic forces. A particle j with charge e_j and mass m_j experiences a scalar potential,

$$U_j = e_j(\Phi - \mathbf{A} \cdot \mathbf{v}_j) \quad (2.23)$$

and hence the system is described by the Lagrangian

$$L = \sum_{j=1}^N \left(-m_j c^2 \sqrt{1 - \beta_j^2} - e_j(\Phi - \mathbf{A} \cdot \mathbf{v}_j) \right), \quad (2.24)$$

where $\beta^2 = \mathbf{v}_j \cdot \mathbf{v}_j/c^2$ [goldsteinClassicalMechanics2013]. The generalised momentum corresponding to coordinate x_j is

$$p_{j,x} = \frac{\partial L}{\partial \dot{x}_j} = m_j \dot{x}_j + e_j A_x, \quad (2.25)$$

explicitely, the generalised momentum describes both the linear mechanical momentum and the momentum of the electromagnetic field. Via Noether's theorem, if L is independent of x_j , *i.e.* spatially homogeneous along x for particle j , then

$$\dot{p}_{j,x} = 0. \quad (2.26)$$

Considering a p-polarised Gaussian laser pulse, axis of polarisation along x , A_x will be approximately constant. Integrating and noting that initially there is no linear or electromagnetic momentum, the generalised transverse momentum conservation equation for an electron at the plasma-vacuum boundary is obtained, namely,

$$p_T = eA, \quad (2.27)$$

where $p_{\text{mathrm}T}$ is the electron momentum along the polarisation axis of the laser pulse. and A its vector potential.

Note that this is only valid provided the radiating electron does not radiate along the direction of \mathbf{A} as discussed by Sokolov *et al* [sokolovDynamicsEmittingElectrons2009]. But we do know this radiation is specular so this is true for normal incidence but not specular?? Really need to consider what the EM fields are in the surface from combined Incident and reflected. The implications of this should maybe be considered?? Also note that this is only true for gaussian pulses with spatial profiles \gg than electron trajectories (*i.e.* twice the relativistic larmor radius).

2.1.1 ZVP electron bunch energies

In [baevaZeroVectorPotential2011], Baeva *et al* propose energy scalings for electron bunches produced in the ZVP regime as a function of the laser intensity and plasma density, finding that one of the key statements of similarity theory ($p \sim a_0 S^x$, where x is some integer value, THIS NEEDS A CITE I THINK IT APPEARS IN BAEVAS ORIGINAL HHG PAPER) holds for the ZVP mechanism. Later this was then extended to three-dimensions (3D) by Savin *et al* [savinAttosecondscaleAbsorptionExtreme2017]. What follows is that discussion with a more close consideration of the both consequences and constants of proportionality.

(Perhaps I should redo this discussion condering infinitessimal areas of the plasma surface to show how variation can exist across the surface) Defo do this! And say that provided the variation is small, rel to what though? the surface remains approximately flat -> that is totally not true

Consider again the semi-infinite block of plasma proposed in figure 2.1, normally irradiated by a laser pulse with wavelength λ_L and peak electric field, E_L . It is now the ponderomotive pressure of the laser that displaces the electron fluid. Consider ust one laser cycle. The electron surface moves inwards until the pressure exerted by the peak instantaneous ponderomotive pressure of the laser pulse cycle,

$$\mathbf{P}_L = \epsilon_0 E_L^2 \hat{\mathbf{x}} = \epsilon_0 \left(\frac{a_0 \omega_L m_e c}{e} \right)^2 \hat{\mathbf{x}} \quad (2.28)$$

is equal and opposite to the pressure exerted by the pseudo-capacitor field,

$$\mathbf{P}_C = \frac{QE}{\sigma} \hat{\mathbf{x}} = -\frac{(en_e \Delta x)^2}{\epsilon_0} \hat{\mathbf{x}} \quad (2.29)$$

using equations 1.8 and 1.9. Equating the magnitudes of \mathbf{P}_L and \mathbf{P}_C , the maximum displacement inwards of electrons is

$$\Delta x \hat{\mathbf{x}} = \frac{c}{\omega_L} \frac{a_0}{\bar{n}_e} \hat{\mathbf{x}} = \frac{1}{kS} \hat{\mathbf{x}}, \quad (2.30)$$

where k is the wave-vector of the laser pulse. Correspondingly,

$$E = \frac{en_e}{\epsilon_0} \Delta x = \frac{\omega_L c m_e a_0}{e} = E_L. \quad (2.31)$$

Applying the results of equations 2.30 and 2.31, when the ponderomotive pressure vanishes and the electron bunch is launched across the pseudo-capacitor, the relativistic kinetic energy gained by a single electron is

$$T = \int \mathbf{F} \cdot d\mathbf{s} = \int_{\Delta x}^0 -eEdx = \int_{\Delta x}^0 -\frac{en_e x}{\epsilon_0} dx = \frac{1}{2} m_e c^2 \frac{a_0^2}{\bar{n}_e} \quad (2.32)$$

or an electron gamma factor,

$$\gamma = \frac{1}{\sqrt{1 - \beta^2}} = 1 + \frac{a_0^2}{2\bar{n}_e}. \quad (2.33)$$

Assuming all displaced electrons are captured by the pseudo-capacitor field and launched as a coherent bunch, the total kinetic energy of the electron bunch is

$$U_{\text{ZVP}} = n_e \sigma \Delta x T = \frac{\sigma n_e}{k} \times m_e c^2 \frac{a_0^3}{\bar{n}_e}. \quad (2.34)$$

It is now interesting to compare equation 2.34 to the laser energy deposited upon the plasma surface and therefore consider what fraction of the laser energy can be absorbed via the ZVP mechanism. Using $E = E_L$, 2.34 can be rewritten as

$$U_{\text{ZVP}} = \frac{1}{2\omega_L S} \sigma c \epsilon_0 E_L^2. \quad (2.35)$$

For the case of normal incidence, bunches are produced at a frequency of $2\omega_L$, naturally following the frequency of the $\mathbf{J} \times \mathbf{B}$ force. Assuming a sinusoidal plane wave incident with surface area σ , the energy absorbed in half a laser cycle is

$$U_{L,1/2} = \sigma \frac{T}{2} \langle I_L \rangle = \frac{2\pi}{4\omega_L} \sigma c \epsilon_0 E_L^2. \quad (2.36)$$

Hence,

$$\eta_{\text{ZVP}} = \frac{U_{\text{ZVP}}}{U_{L,1/2}} = \frac{1}{\pi S}. \quad (2.37)$$

Interestingly, this new analytical result predicts the trend observed by A. Savin [**savinModellingLaserPlasmaInteractions2019**] in **PIC!** simulations both in magnitude and in scaling. Indeed, A. Savin demonstrated

$$\eta_{\text{ZVP}} \sim S^{-1.000(3)}, \quad (2.38)$$

however, this result led A. Savin to conclude increasing S increases the energy in the reflected High Harmonic Generation (HHG) beam thus increasing high harmonic efficiency, seemingly in tension with the vast majority of the work on this regime [CITE CITE CITE]. The resolution arises from the following: there are two distinct conversion efficiencies which describe the reflected harmonic spectrum: the conversion efficiency into the whole reflected beam and the conversion efficiency into individual harmonics. While the total conversion into the reflected beam decreases for decreasing S , the slope of the harmonic spectrum also decreases and

therefore while A. Savin is absolutely correct, the important parameter (the slope of the harmonic spectra) follows the opposite trend.

Indeed high X-ray harmonic efficiency necessitates high inefficiencies in the production of ZVP electron bunches as higher energy bunches produce more coherent reflected radiation, a caveat not often considered in the quest for higher-order harmonics.

[Side note for my reference: bunch is made and at peak compression at peak of laser pulse. then laser field oscillates, inside the bunch they experience an $a_0 = 0$ (? maybe) outside there is a minimum in the field, then the bunch is rotated back when it hits the next peak of the laser pulse (ie $a_0=0$? outside plasma?) the upshot of this is I can then say there is a distance of $\lambda/2$ between bunch peak displacement and radiation point and since peak displacement = $1/kS$, for all S , the pseudocapacitor has been completely discharged and therefore there has been the maximum energy gain before HHG production - important for electron bunch gamma factor discussion.]

Next up: the unification of RES and ZVP.

2.1.2 ZVP bunches oblique incidence scaling and internal bunch structure

This section is inspired by [gonoskovUltrarelativisticNanoplasmonicsRoute2011] and [vincentiOpticalPropertiesRelativistic2014] supplementary material but different where I believe they have gone wrong to generalise the ZVP mechanism energy scalings.

The below section needs cleaning up of minus signs etc, take the convention laser propagates in the positive direction therefore drift of electrons and ions in frame with normal incidence is in negative direction.

As has previously been stated, if the plasma-vacuum boundary is sufficiently steep, the plasma electrons will respond adiabatically to the laser pulse and arrange themselves to form a pseudocapacitor longitudinal electric field E_C at the plasma surface. At all points in this adiabatic phase, the surface electrons will be in a

quasi-static equilibrium *i.e.* there will be a balance between the electromagnetic forces on them. Consider again a laser pulse incident on a solid density plasma existing for $x > 0$ at angle θ . Transforming to the reference frame where the laser is incident normally (quantities in this frame are indicated by the primed symbol), the electron and ion bulk plasma species are now streaming with a velocity $\mathbf{v}_d = -c \sin \theta \hat{\mathbf{y}}$. From the Lorentz force law along the longitudinal direction ($\hat{\mathbf{x}}$), for a displacement of the electron fluid x'_e (one assumes that the expression for a single electron at the surface describes the surface as via relativity all electrons follow similar trajectories), travelling at speed \mathbf{v}'

$$-e(\mathbf{v}'(x'_e) \times (\mathbf{B}'_L(x'_e) + \mathbf{B}'_i(x'_e)) \cdot \hat{\mathbf{x}} + E'_C(x'_e)) = 0, \quad (2.39)$$

where

$$B'_L = \frac{m_e \omega'_L a_0 \sin(\omega'_L t' - k' x'_e)}{e} \hat{\mathbf{z}} \quad (2.40)$$

and B_i originates from the uncompensated ion current, $\mathbf{J}_i = Z e n'_i(x'_e) \mathbf{v}_d$, where the electron fluid has been displaced. As before, from equation 1.9,

$$E'_C = \frac{en'_e x'_e}{\epsilon_0}. \quad (2.41)$$

Note that there is no contribution to the laser magnetic field here from the reflected laser pulse since the assumption is that during this pushing phase all laser pulse energy is converted into electrostatic potential energy, this is supported by the attosecond duration of the reflected harmonic beam (*i.e.* it is not produced during this phase). Maxwell-Ampère's Law states

$$\nabla \times \mathbf{B} = \mu_0 \mathbf{J}. \quad (2.42)$$

Noting that by symmetry there can be no variation in the magnetic field with y' or z' it becomes clear that

$$-\frac{d(\mathbf{B}'_i)_{z'}}{dx'} = \mu_0 (\mathbf{J}_i)_{y'}. \quad (2.43)$$

Integrating equation 2.43 from $-\infty$ to x'_e , noting that $\mathbf{B}_i = 0$ at infinity and assuming a constant density profile n'_i for $x > 0$,

$$\mathbf{B}'_i(x'_e) = \mu_0 e n'_e x'_e c \sin(\theta) \hat{\mathbf{z}}. \quad (2.44)$$

Using equations 2.40, 2.41 and 2.44 and making the very reasonable approximation that the relativistic electrons on the surface move at speed $v'_y \approx \pm c$ at peak displacement ($x'_e = x'_p$), 2.39 can be written as

$$-e \left(\pm c \left(\pm \frac{m_e \omega'_L a_0}{e} + \mu_0 e n'_e x'_p c \sin \theta \right) + \frac{en'_e x'_p}{\epsilon_0} \right) = 0. \quad (2.45)$$

Note that to be in the laser pushing phase the first term must be negative, corresponding to \mathbf{v}' and \mathbf{B}'_L having the opposite sign, hence,

$$c \left(-\frac{m_e \omega'_L a_0}{e} \pm \mu_0 e n'_e x'_p c \sin \theta \right) + \frac{en'_e x'_p}{\epsilon_0} = 0, \quad (2.46)$$

where here the \pm tracks the sign of \mathbf{v}' . After some manipulation, one arrives at

$$x'_p = \frac{1}{k' S' (1 \pm \sin \theta)}. \quad (2.47)$$

Transforming back to the lab frame, naturally,

$$x_p = \frac{1}{k S (1 \pm \sin \theta)}. \quad (2.48)$$

Already this is quite a result, reducing to equation 2.30 for $\theta = 0$ and predicting the suppression and enhancement of the two surface oscillations per laser pulse cycle. Explicitely, for a laser pulse propagating at $y = x \tan \theta$, the peak displacement of the electron surface is enhanced for \mathbf{B}_L in the $+\hat{\mathbf{z}}$ -direction and suppressed for \mathbf{B}_L in the $-\hat{\mathbf{z}}$ -direction.

Consider now acceleration of the electron bunch across the pseudocapacitor field in the boosted frame,

$$T' = \int \mathbf{F}' \cdot d\mathbf{s}' = \int_{x'_p}^0 -e E'_C(x'_e) dx'_e = \frac{en'_e (x'_p)^2}{2\epsilon_0} = \frac{1}{2} m_e c^2 \frac{a_0^2}{\bar{n}'_e (1 \pm \sin \theta)^2}. \quad (2.49)$$

Again, transforming back to the lab frame, noting the gain in energy from crossing the pseudo-capacitor

The linearity of four-vectors ensures

$$\Delta \mathbf{P}^\mu = \left(\frac{\Delta E}{c}, \Delta \mathbf{p} \right) \quad (2.50)$$

is also a four-vector. The Lorentz transform for change in energy is thus

$$\Delta E = \gamma \left(\Delta E' - \frac{\mathbf{v}_d}{c} \cdot \Delta \mathbf{p}' \right), \quad (2.51)$$

where

$$\gamma = \frac{1}{\sqrt{1 + \sin^2 \theta}} = \frac{1}{\cos \theta}. \quad (2.52)$$

Hence for energy gain $\Delta E' = T'$ in the boosted frame (where $\Delta p_y = 0$),

$$T = \gamma T'. \quad (2.53)$$

Using equations 2.49 and 2.52 and recalling $\bar{n}_e = \bar{n}'_e / \gamma$,

$$T = m_e c^2 \frac{a_0}{2S(1 \pm \sin \theta)^2} \quad (2.54)$$

Nb this could have simply been established in the lab frame and considering $F.ds$ which is just the same[The electron bunch then accelerates across the pseudo-capacitor in the specular direction, the force] maybe put this derivation in appendix.

Also note that when doing this transformation, T is the energy gained but there is another term in the momentum from the transform, since now $v_y = c \sin \theta$. This is unrelated to the energy gain from crossing the pseudo capacitor. There is no explanation of where this energy comes from, just that in order for the bunch to travel in the $-x$ direction in the boosted frame - not sure what real explanation there is for this to occur, also confusion here since is this actually contained within the gamma expression or not, im lost come back to this. Maybe actualyl this is fine. We jsut take the gamma factor associated with the py gain ($= \sec \theta$ - corresponding to a gamma of 1.4 at 45 degrees) and add the delta gamma from the pseudo capacitor and that should be fine.

Another note: this dependence on theta ($1 \pm \sin \theta$) can be explained as an increase due to the electric field having a component acting either in or out from the plasma surface either assisting or counteracting the magnetic field.

Idea: Can one use an external constant magnetic field to obtain the same results for normal incidence?

Also need to go back through this section and make clear which gamma is which in this section

Therefore, as with peak displacement, the energy gained by the electron bunch via the ZVP mechanism is suppressed in one half cycle and enhanced in the second.

While this model would suggest an optimal angle for electron energy and therefore HHG of $\pi/2$, if $\theta > \pi/4$, then, if the relativistic electron bunch is travelling at c along the specular reflection direction, the subsequent laser peak amplitude will never ‘catch up’ with the electron bunch, and electrons will escape through the antinodes (?) of the electric field [CITE KRUSHELNICK PAPER GRAZING INCIDENCE ELECTRONS], generating high charge electron bunches in reflection, but decreasing **HHG efficiency!** (**HHG efficiency!**).

Finally, moving on to the calculation of total bunch energy as a function of θ . Since the total number of electrons in the accelerating bunch must be invariant,

$$U_{\text{ZVP}}(\theta) = n_e \sigma \Delta x T(\theta) = \frac{\sigma n_e}{k} \times m_e c^2 \frac{a_0}{2S^2(1 \pm \sin \theta)^3}. \quad (2.55)$$

What we can see from this is this enables a larger fraction of the laser energy to be absorbed at high S pushing the currently experimentally accessible regime into the most efficient regime.

I want to move on, but return to this section and sort out the following.

Another concern: peter showed me sims that suggested that increasing S increased the suppressed oscillations more RELATIVE to the main oscillations, perhaps need to look at the internal bunch structure?

Also see if can do a second order calculation through the electron bunch to see if can calculate its structure.

Big note: The highest electron gamma factors comes from those electrons at the very front surface who are accelerated before high density is reached and quasistatic equilibrium reached (there are therefore very few of them), these few electrons do not satisfy ZVP relation for energy, instead ponderomotvie + ZVP which at most would be twice the predicted gamma which is quite some difference

HOWEVER for all experiments so far, ZVP energy gain is small since S large so ponderomotive is more sensible.

Earlier write something along the lines of explaining while ZVP absorption does represent laser energy absorption, bulk heating occurs rather indirectly.

2.2 Defining characteristics of the ZVP mechanism

In her original paper, T. Baeva *et al* [**baevaZeroVectorPotential2011**] outlined 6 defining characteristics of the ZVP mechanism, namely,

1. The existance of vector potential zeros moving through the skin layer in the laboratory frame;
2. The existance of zeroes in the incident laser pulse vector potential required for the formation of fast electron bunches;
3. The generation of fast electron bunches with ultra-short temporal duration;
4. Such bunches should be described by the expressions for average 2.54 and total energy 2.55;
5. An intrinsic link must exist between the fast electron bunches and coherent X-ray HHG;
6. Injection of the fast electron bunches along the propagation axis of the laser pulse;

with the essential point being it is the moving zeros within the skin layer being the defining delineator between this post-ponderomotive regime of laser pulse energy absorption and all other proposed mechanisms. While such observational requirements are far beyond the reaches of currently experimental know-how, numerical simulations in both 1- [**baevaZeroVectorPotential2011**] and 2-dimensions [**savinAttosecondscaleAbsorptionExtreme2017**] have confirmed the above points. Now is presented the first 3D simulations to demonstrate the ZVP mechanism.

2.3 Numerical simulations of the ZVP mechanism

This thesis relies throughout on the analysis of 1,2 and 3D **PIC!** simulations, primarily using the massively-parallel and open-source simulation code Smilei [derouillatSmileiCollaborativeOpensource2018]. Simulation parameters will be provided throughout.

2.3.1 The ZVP mechanism in 3D

Results are presented in figure 2.2.

Discuss choice of S parameter somewhere. Also note that these parameters are currently accessible on ELI-NP.

I will finish this section once the results of the rest of the 3D sim stuff is done. One thing to remark:

The remarkable similarity between the 2 and 3D simulation results is a natural consequence of the 2D nature of the interaction geometry. It is however still reassuring to note that previous work withstands this stringent test of the real universe.

(At some point list all the other sources of potential error, including ignoring ionisation, ionisation states, collisions.)

Interesting result of the 3D sim: Can see bunch on front surface and laser clearly propagating behind it. Is this since in this new regime (ZVP dominating HHG) the thin bunch barely attenuates (ie reflects) the laser pulse when it is accelerating across the pseudo capacitor, hence the laser is still effectively able to compress the plasma surface and keep the process going. Meanwhile the reflected HHG light comes mostly from converting bunch KE into HHG.

Convergence of 3D simulations

The 3D simulation parameters were chosen to be consistent with previous work on the ZVP mechanism, however, such simulations are cumbersome, limiting the number of simulations it is feasible to run. Certainly parameter scans are not currently available. In order to query the defining characteristics outlined by Baeva, a smaller simulation was run with similar parameters to the initial simulation (this

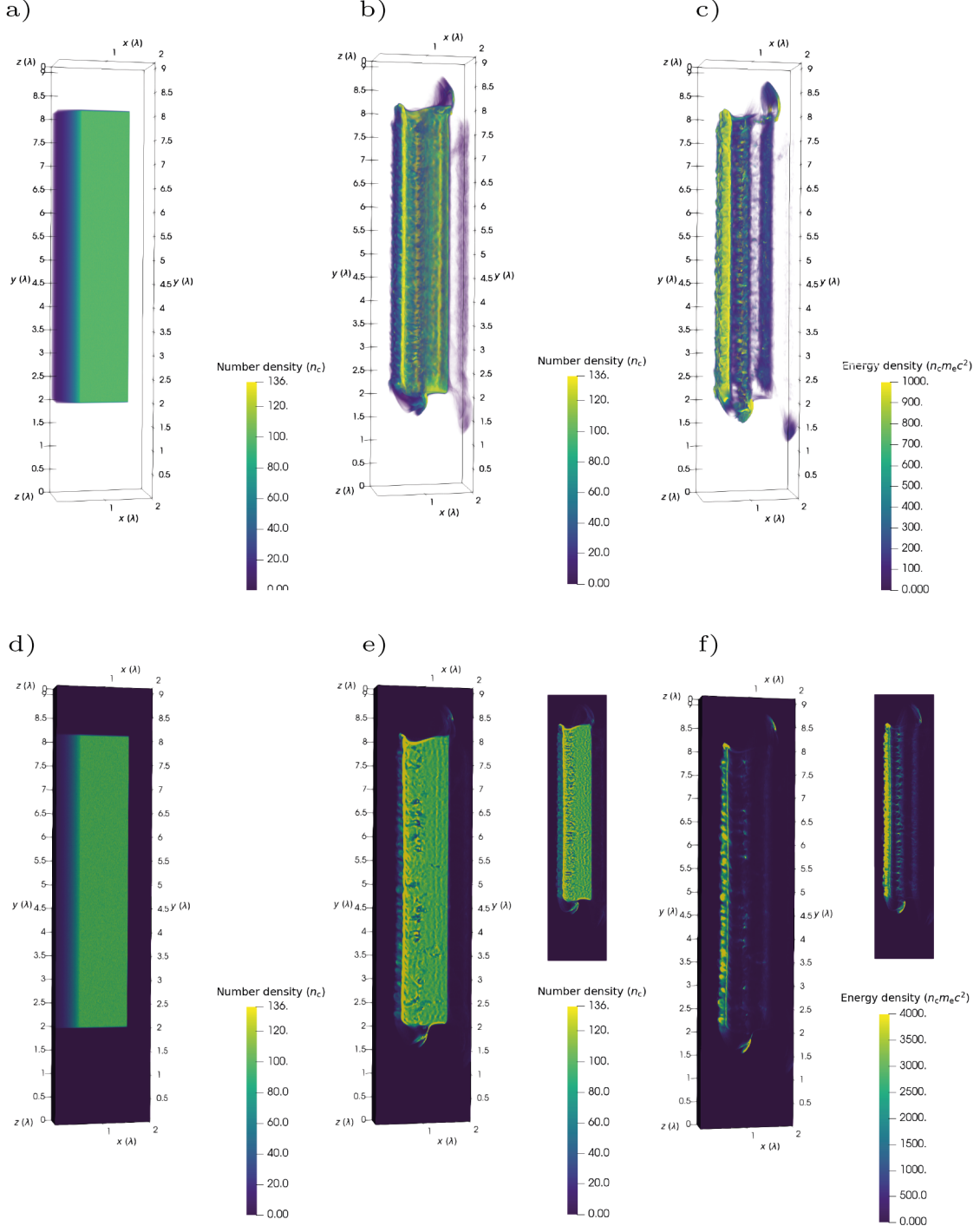


Figure 2.2: Simulation results from a 3D PIC! simulation of the ZVP mechanism. a) The initialised electron number density. b) The electron number density several cycles later, the plasma bulk is intact, however there is evidence of instabilities and electron bunches propagating through and around the plasma. c) The electron kinetic energy density at the same timestep. Note that the scale has been clipped to enable observation of both electron bunches propagating through and around the plasma bulk. Significantly higher energy density, corresponding to a higher charge density and attosecond duration for the electron bunches propagating around the bulk. d-f) Plots clipped through $z = 0$ for a-c) respectively for better clarity on the internal structure of the plasma bulk. The accompanying plots for figure e) and f) are corresponding 2D PIC simulation results.

is 9/18 compare) but at lower resolution. The two simulations are compared in figure 2.3. Good convergence is qualitatively demonstrated by the presence of characteristic features of the ZVP mechanism. While the instabilities are similar in structure, the change in seeding changes their exact positions. As instabilities are not the focus of this thesis this variation is of no concern.

Maybe mention somewhere that I would also add pseudocapacitor field as an essential characteristic of the ZVP mechanism that should generally be identified.

Following the success in reproducing the key features of the ZVP mechanism and demonstrated consistency between 2 and 3D equivalent simulations, the remainder of this chapter will predominantly utilise 2D simulations to interrogate the mechanism further.

2.3.2 The ZVP electron bunch

Although much has been stated of the high energy and short duration of ZVP electron bunches in the previous work, until now much of the quantitative discussion of the properties of such bunches has avoided interrogation. A ZVP electron bunch is an electron bunch produced via the ZVP mechanism. Once produced and accelerated across the pseudocapacitor field, it is launched back in the laser propagation direction. While the bunch has no spatial separation over energies when propagating with the zero of the vector potential, the turning point of the electrons is longitudinal momentum dependent due to the Coulomb attraction of the ions after overshooting the pseudocapacitor field. Baeva *et al* showed that the electron bunch has a quasi-monoenergetic spectrum: there is a one-to-one relationship between energy and position with the higher energies trailing the lower energies. The full bunch is confined to 130 as while a single energy confined to 5 as. If, however, the plasma bulk is transversely mass-limited relative to the laser spot size, when rotated back towards the plasma block, some of the electron bunch will overshoot and escape the potential well without significant stretching of the bunch in time as can be seen in figure 2.2. Such electron bunches (retain the initial energy spread???? ie fast first as discussed in RES paper) retain their high charge density and ultra-short duration.

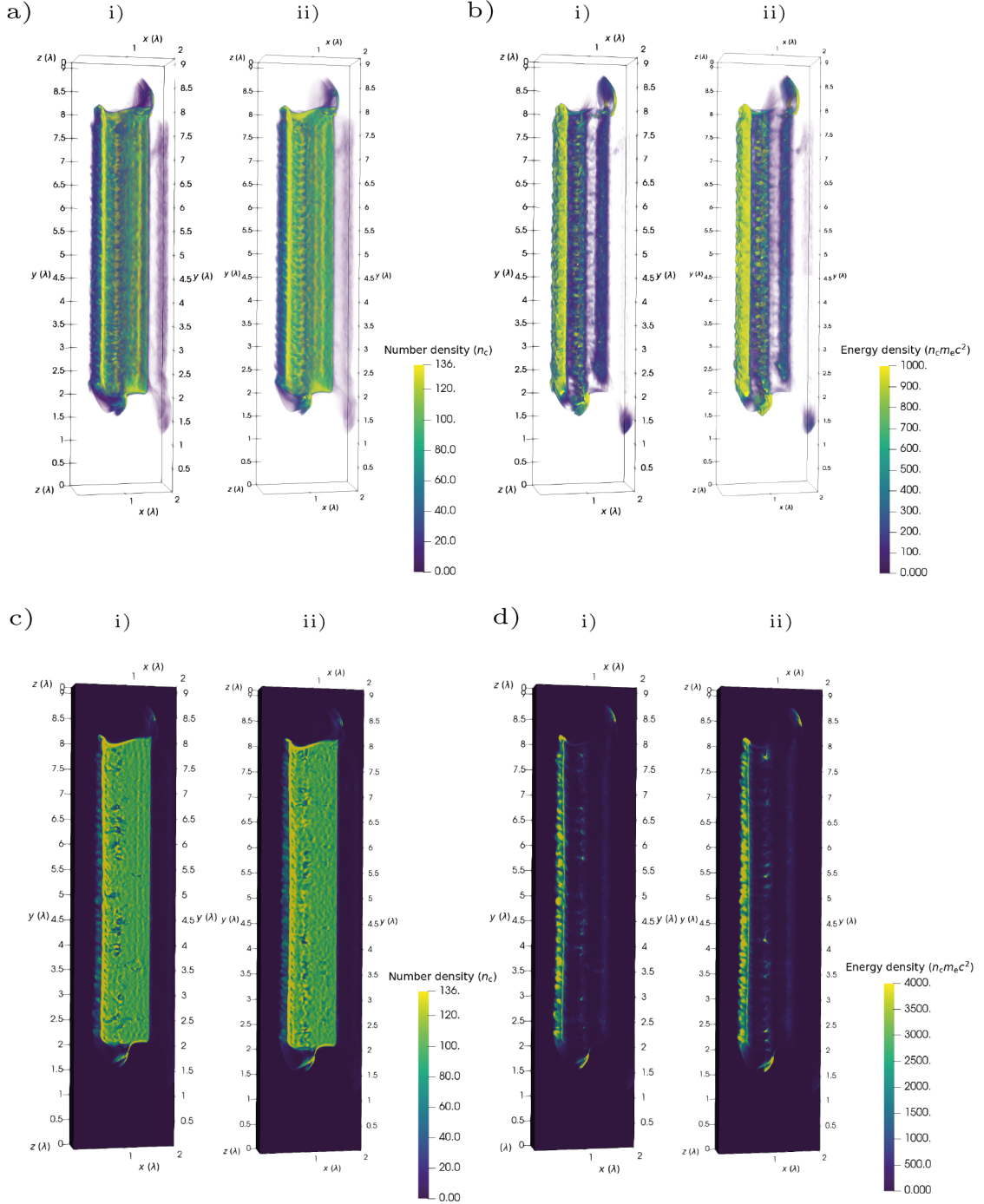


Figure 2.3: Comparison between the initial 3D simulation and a lower resolution version. a) Electron number density. b) Kinetic energy density. c) and d) are slices of a) and b) respectively. *i*) Initial simulation. *ii*) Lower resolution simulation. Good convergence is demonstrated.

ZVP electron bunches can therefore be placed into two categories: ultra-high charge, ultra-short duration electron bunches from mass-limited targets, hereafter labelled mass-limited electron bunches, of interest due to their unique properties and bulk propagating bunches, hereafter labelled bulk bunches, which have lower charge densities, are imprinted with instabilities and are instead of interest due to their connection to energy absorption and reflection in this post-ponderomotive regime.

To investigate these two bunch types further, 2D PIC simulations were performed, see appendix for parameters. Figure blah is representative.

Attosecond nano-Coulomb mass-limited electron bunches

Figure 2.4 describes a typical mass-limited ZVP electron bunch qualitatively. The electron bunch under interrogation is ultra-relativistic with a mean energy of 51(11) MeV and a duration of 35 as. It propagates at an angle of -393 rad relative to the laser propagation direction, *i.e.* the x -axis, and a transverse geometric emittance in the simulation plane (the x - y plane) of 35(7) nm rad. A definition of the transverse geometric emittance, a measure of the quality of the electron beam, is given in appendix A.1. Note that while the bunch does not propagate in the laser propagation direction, this does not mean it must be rejected under consideration of the ZVP bunch conditions. Indeed, the bunch must propagate at some angle to the laser since conservation of canonical momentum while it remains in thrall of the laser pulse it must have some transverse component of momentum. The more standard ZVP bunches passing through the bulk again by conservation of momentum must propagate along the axis, as is observed in simulation. For an equivalent bunch in a corresponding 3D simulation, the transverse geometric emittance in the z plane is 15(11) nm rad. This electron bunch has a total charge of 0.35 nC for a slab of plasma of thickness 0.75λ in the z -direction. Noting again the two-dimensional nature of the interaction geometry, and that electrons less than twice the relativistic Larmor radius,

$$r_l = \frac{\gamma m_e v}{e B}, \quad (2.56)$$

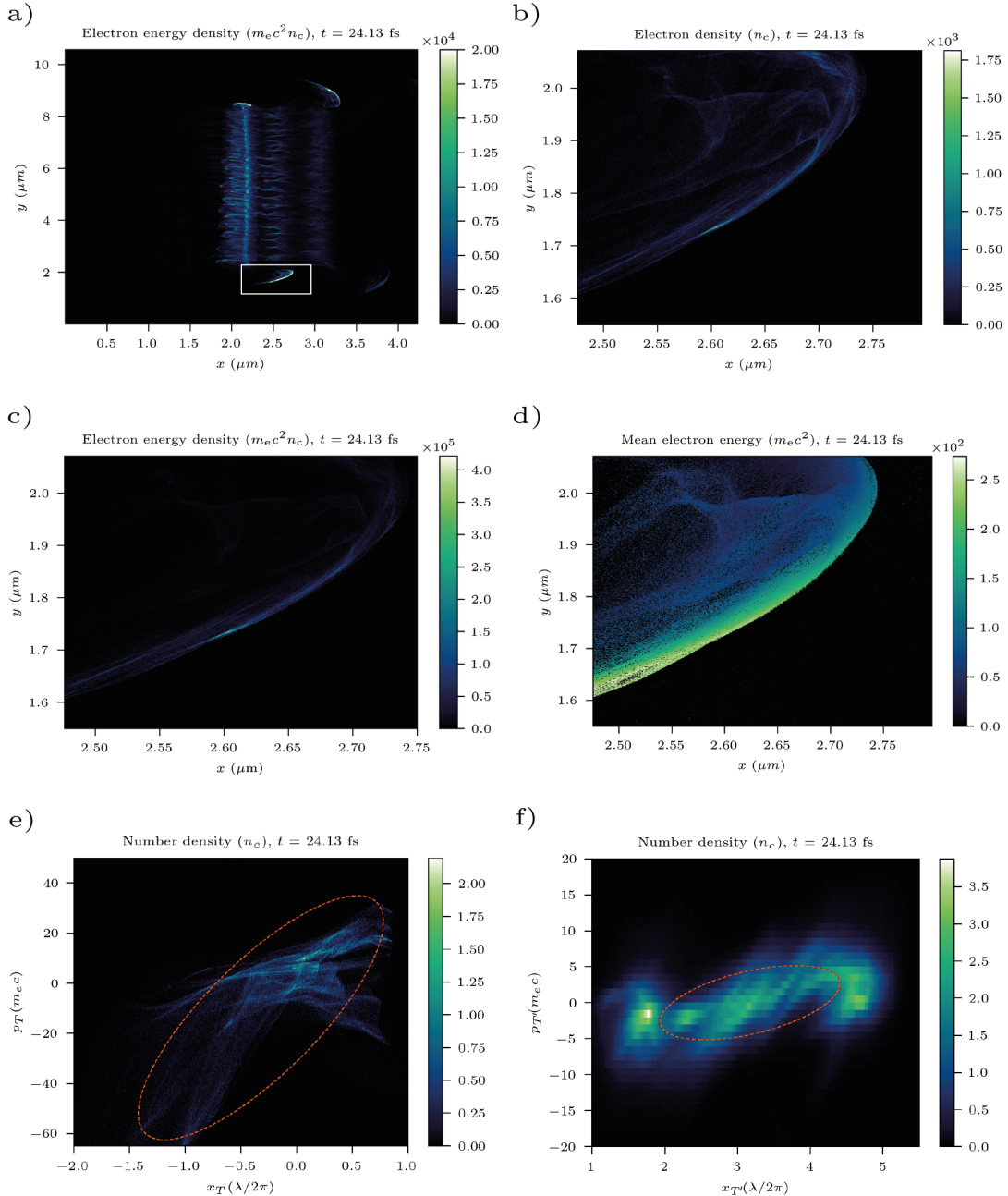


Figure 2.4: 2D PIC simulation results qualitatively describing typical mass-limited ZVP electron bunch structure. a) Electron energy density for the full simulation window, corresponds to figure 2.2f). The box highlights the bunch presented in the following plots. b) Electron number density of the electron bunch. c) Electron energy density of the electron bunch, the colourbar scale has been increased compared to figure a) to demonstrate the internal structure. d) The mean electron energy across the electron bunch, suggesting a position dependent energy or quasi-monoenergetic nature to the electron bunch [baevaZeroVectorPotential2011]. Cells with no macroparticles are black. e) The transverse phase space in the 2D simulation plane. The ellipse describes the calculated emittance. The skew of the ellipse is a consequence of a low density tail on the phase space beyond the bottom left corner. f) This plot was extracted from the equivalent 3D simulation and describes the transverse emittance in the z -direction. Again the ellipse marks the emittance. The relatively well-defined border to the phase space and the mild tilt (indicating only mild divergence) are direct consequences of the 2D nature of the interaction.

where γ and v correspond to the electron velocity and B is the magnetic field of the laser pulse, when rotated back towards the plasma will escape to the side, the total number of electrons in the mass-limited bunch is

$$N = 2n_e r_l L_z \Delta x, \quad (2.57)$$

where L_z is the width of the plasma in the z -direction. Using equation 2.30 for Δx and 2.52 for γ and approximating $v \approx c$ for the ultra-relativistic electron bunch,

$$N = 2\gamma n_c \frac{L_z}{k^2}. \quad (2.58)$$

For these simulation parameters, this corresponds to a total bunch charge, $Q = eN$, of 0.37 nC, a remarkably successful prediction of the ZVP model. Equation 2.58 tells us there is no limit to the

Equation 2.58 can be rewritten in terms of fundamental constants as

$$N = 2(1 + 0.5 \frac{a_0^2}{\bar{n}_e}) L_z \frac{m_e \epsilon_0 c^2}{e^2}. \quad (2.59)$$

Almost counterintuitively, it would appear the total charge scales inversely with the plasma density. Instead, charge can be increased either by increasing the laser pulse intensity or L_z . Indeed, provided the laser pulse intensity remains relativistic, the focal spot can be increased indefinitely and there is no limit to the mass-limited electron bunch total charge. For a realistic laser pulse with beam width 10λ incident on a larger laser block, equation 2.59 predicts a charge of 9.3 nC.

Discuss use cases of the electron bunches. DIscuss if bunch quasi-monoenergetic.

Figure blah blah compares the electorn bunch energy to an equivalent¹ bunch produced by a circularly polarised laser pulse. The mean electron bunch energy is over three times lower as there is no ZVP acceleration phase and there is no quasi-monochromatic nature [**baevaZeroVectorPotential2011**].

¹A circularly polarised laser pulse will expel electrons from a mass-limited target in a corkscrew shape, the bunch is therefore only loosely equivalent.

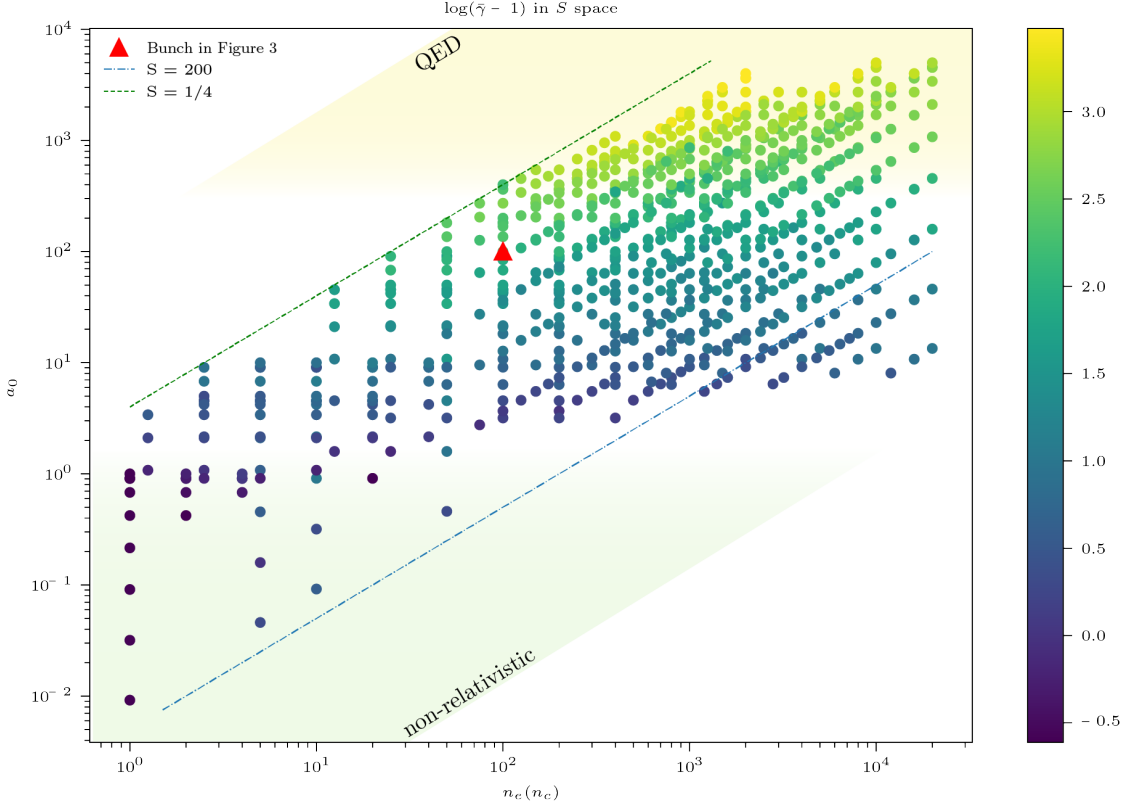


Figure 2.5: Mean mass-limited ZVP electron bunch normalised kinetic energies extracted from 2D PIC simulations. The bunch detailed in figure 2.4 is highlighted.

Parameter scan of electron bunch mean energy

Since ZVP energy scaling is a fundamental identifier of ZVP bunches, it is important to confirm that mass-limited electron bunches follow the same scaling relations as has previously been confirmed for bulk ZVP electrons in both 1D [baevaZeroVectorPotential2011] and 2D [savinAttosecondscaleAbsorptionExtreme2017] PIC simulations. The mean mass-limited electron bunch kinetic energies were extracted from 120 2D PIC simulations and are plotted in figure 2.5. The dependence on both a_0 and n_e demonstrates these electron bunches are accelerated by a non-ponderomotive mechanism. The parameter scan ranged plasma block density ranging from the critical plasma density to well-beyond solid density for the aluminium target and with laser pulse peak intensity ranging from non-relativistic ($a_0 < 1$) through to the **QED!** (**QED!**) plasma regime ($a_0 > 300$) up to a peak $a_0 = 5000$ to investigate the change in scaling observed by Savin *et al*

[**savinEnergyAbsorptionLaserQED2019**] at the onset of QED effects. This study is also the first to extract specific bunch energies as opposed to total simulation box energy gain, representing a far more stringent test of ZVP theory.

Care must be taken however as the energy of such electron bunches cannot be directly compared to the ZVP energy relations as as aforementioned after escaping the potential, the electron bunch experiences further direct laser acceleration before reaching the detection point. Indeed, Thévenet *et al* [**thevenetVacuumLaserAcceleration2016**] suggested that attosecond electron bunches produced in reflection exhibit precisely the phase and energy properties required to ‘surf’ the reflected laser pulse and experience vast acceleration gradients over the Rayleigh length of the laser pulse. This process is known as Vacuum Laser Acceleration. It seems highly likely that this process occurs for electron bunches produced in transmission. This seemingly unfortunately situation in reality provided a fully optical scheme to create GeV nano-Coulomb electron bunches from the most simple of setups: a laser interacting with a mass limited solid target (thus reducing the alignment complexity.).

Returning to the determination of the electron bunch energy at the measurement point, consider now the journey of the electron bunch after expulsion from the plasma bulk. It is rotated back towards the plasma bulk by the magnetic field of the subsequent peak of the laser pulse, then travelling at approximately c it surfs the peak, experiencing an approximately constant accelerating electric field from the laser pulse at some fraction f of the laser field peak. The work done by this field is then

$$\Delta T = \int e\mathbf{E} \cdot d\mathbf{x}. \quad (2.60)$$

Note that for this process, the laser pulse electric field and electron bunch direction of travel will always be aligned no matter to which side of the plasma bulk the electrons are accelerated to and therefore ΔT will always increase the energy of the electron bunch, thus,

$$\Delta T = efE_L\Delta y, \quad (2.61)$$

where Δy is the distance along y from the plasma edge to the detection point. Accounting for the Gaussian spatial profile of the laser, $a(t) = a_0 \exp(-y^2/(6\lambda)^2)$ at focus, the gamma factor after both acceleration phases for this simulation setup is then

$$\gamma = 1 + (0.30) \times \frac{a_0^2}{\bar{n}_e} + (1.2f) \times a'_0. \quad (2.62)$$

Here the primed vector potential refers to the intensity of the subsequent peak of the laser pulse. This final term could be neglected or at least reduced somewhat once super-Gaussian spatial laser pulses become standard in this intensity regime or using a suitable plasma separator [1]. Both acceleration phases fail to meet the criteria of the Lawson-Woodward theorem. The ZVP phase is dependent on the existence of electrostatic forces, while the secondary phase occurs for a finite interaction region.

Fitting equation 2.62 to the PIC simulation data presented in figure 2.5 finds

$$\gamma = 1 + (0.46 \pm 0.02) \times \frac{a_0^2}{\bar{n}_e} + (0.28 \pm 0.01) \times a'_0 \quad (2.63)$$

with an r^2 -value of 0.818. This fit suggests $f = 0.22 \pm 0.01$. The electric field experienced for a random selection of electrons in a bunch was extracted from one simulation. Encouragingly, the mean attenuation of the electric field they experience is 0.20 ± 0.05 , to calculate this attenuation directly falls beyond the scope of ZVP theory.

This is the first demonstration of ZVP theory to calculate actual values and not only the scaling relationship. Such order of magnitude calculation is essential to compare this model of absorption to others and thus determine the dominant mode for absorption. It is certainly remarkable that such a simple theory for energy absorption has such predictive success in this highly non-linear and seemingly chaotic many particle system. It is interesting that increasing laser intensity to such extremes will, at least for a short time, cause relativistic effects that add coherency to electron motion before total annihilation of a target.

The relative error between data and theory is plotted in figure 2.6. Those points marked by an orange triangle have associated errors of over an order of magnitude. Reassuringly, such points occur only after the onset of QED effects,

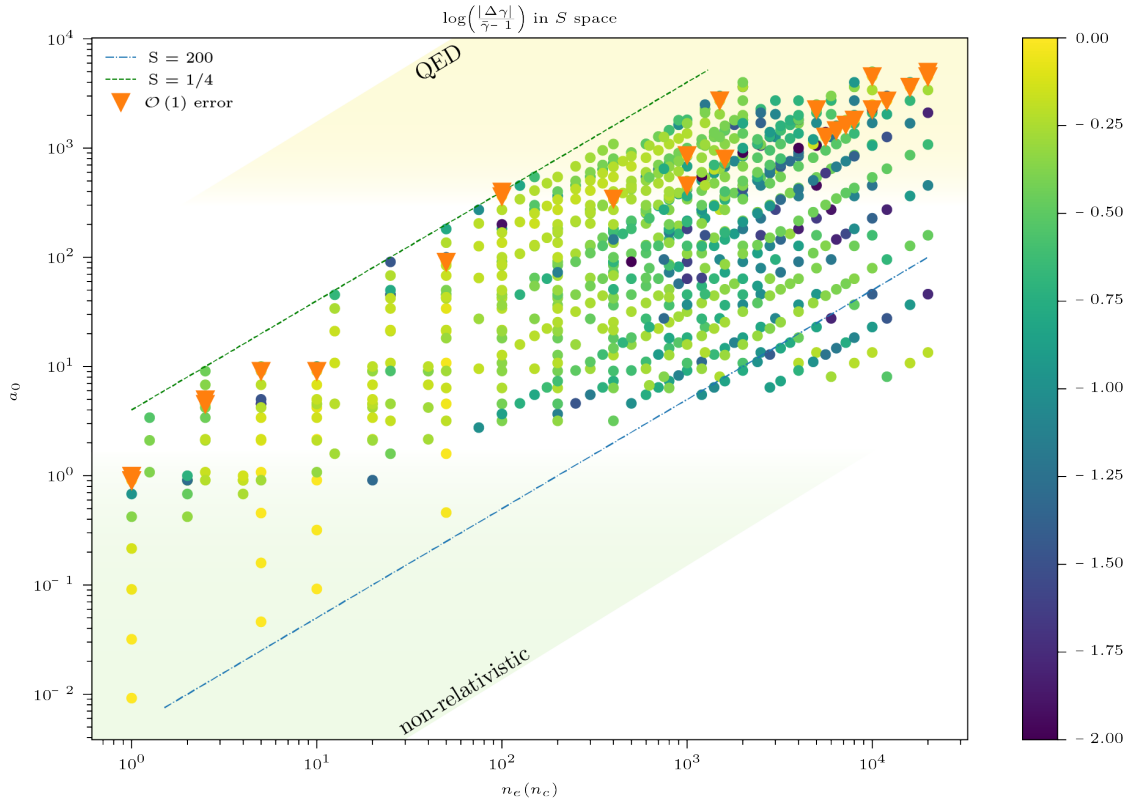


Figure 2.6: The relative errors for each mean energy data point compared to figure 2.5. The orange triangles indicate data points for which the model fails to predict the mean energy.

known to impact the ZVP mechanism [2] and for $S < 1$, that is, where the plasma becomes relativistically transparent to the laser pulse, a fundamentally different regime. Equally, for non-relativistic laser intensities, where assumptions of electron coherency cannot be made, are poorly fit by the model. It is particularly interesting that there is no indication that large S causes a breakdown of the model, extending the applicability of the model further than previously considered, opening up the field to a wider range of conditions, such as that of shock compressed plasmas. To summarise, it would appear the ZVP model is valid for $10 \leq a_0 \leq 300$ and $S \geq 1$.

To do: Look again at trajectories Look again at just fitting the region where expression is valid. Temporal effects (non-existent, discuss)

2.3.3 Total electron bunch energy scaling

Then Energy scalings

Then QED? Then experiment?

To do: convergence of electron bunch energies with nppc and sim resolution.

At some point mention:

Note that ZVP does not describe the peak energies in the bunches, then JxB applies, since there are always some electrons outside of the well defined sharp boundary when the density is not high enough to impose adiabaticity.

3

Miscellaneous notes

Contents

3.1 ORION experiment	37
3.1.1 Frames of reference	37
3.1.2 ORION interaction geometry	41
3.1.3 Condition on validity of hole boring expression	42

3.1 ORION experiment

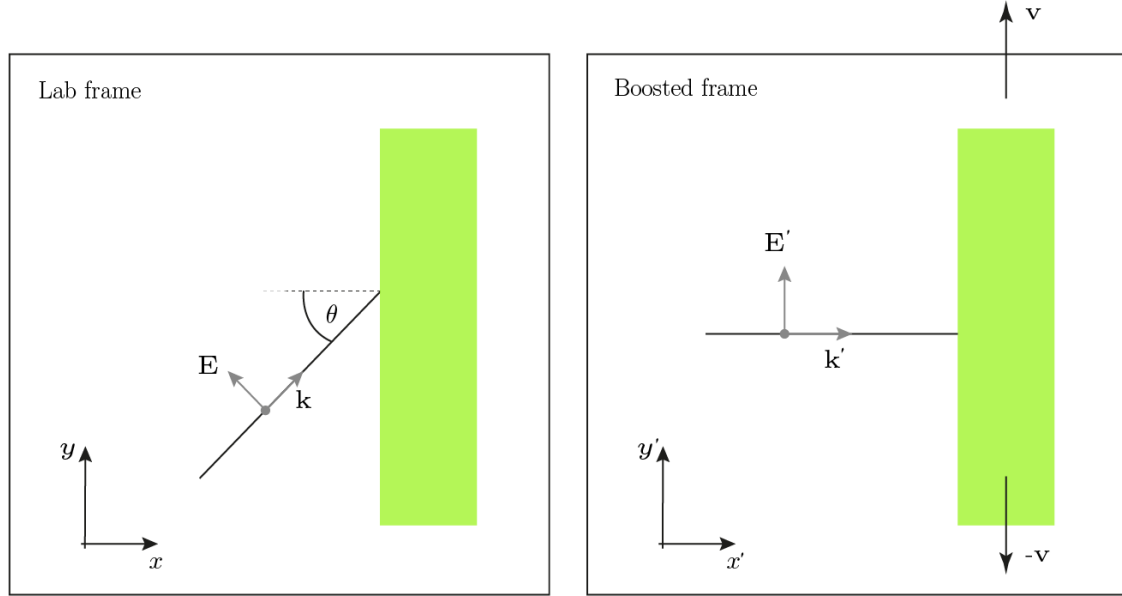
The following derivation determines the polarisation of the ORION laser pulses in the experiment and the boosted frame quantities for the PIC simulations.

I will have a whole subsection devoted to the different frames of reference of relevance and then a second one about normalised units. What follows now is the derivation of the boosted frame in which the laser is incident normally relative to the lab frame where the laser is incident obliquely.

I will try to use a consistent convention for coordinate system as much as possible.

3.1.1 Frames of reference

Other frames of reference include, HB front surface at rest frame, ablating front frame, smilei frames.

**Figure 3.1**

When writing out the pistonning equation in full in thesis, include analysis in Robinson 2009 to do it for multiple ion species.

I should go over this and use third year relativity notes to formalised and make more consistent.

While some of this section may seem trivial, it is frequently miscalculated in the literature, it therefore seems of great importance to provide a full derivation.

Consider a photon incident on a plasma block at angle θ as in figure 3.1. A boost is applied with velocity \mathbf{v} to a frame such that the photon is normally incident on the now streaming plasma at velocity $-\mathbf{v}$. The velocity transformation for the photon's velocity, \mathbf{u} , parallel to the boost is

$$\mathbf{u}'_{\parallel} = \frac{\mathbf{u}_{\parallel} - \mathbf{v}}{1 - \mathbf{u} \cdot \mathbf{v}/c^2}. \quad (3.1)$$

Setting $\mathbf{u}'_{\parallel} = 0$, it is clear that

$$\mathbf{v} = \mathbf{u}_{\parallel} = c \sin \theta \hat{\mathbf{y}} \quad (3.2)$$

in this geometry and

$$\gamma_{\mathbf{v}} = \frac{1}{\sqrt{1 - \mathbf{v}^2/c^2}} = \sec \theta. \quad (3.3)$$

Noting that since Snell's law is frame invariant, the photon remains normal as it propagates into the skin depth of the plasma, a frame in which the interaction reduces to a 1D problem has been successfully found for all $\theta < \pi/2$. Those familiar with the topic may wonder how this is possible considering the ‘ripples’ that are observed on the plasma surface for oblique incidence. The explanation for this is of course the relativity of simultaneity. It remains to determine how do all the relevant quantities transform as such a boost is applied. Starting with an easy one: the photon’s wave four-vector is

$$\mathbf{K}^\mu = \left(\frac{\omega}{c}, \mathbf{k} \right) \quad (3.4)$$

and thus the frequency transforms as

$$\frac{\omega}{c} = \gamma_v \left(\frac{\omega'}{c} - \frac{\mathbf{v}}{c} \cdot \mathbf{k}' \right). \quad (3.5)$$

Since $\mathbf{v} \cdot \mathbf{k}' = 0$,

$$\omega' = \omega \cos \theta. \quad (3.6)$$

As

$$n'_c = \frac{m_e(\omega')^2}{4\pi e^2}, \quad (3.7)$$

$$n'_c = n_c \cos^2 \theta, \quad (3.8)$$

while the plasma block will be Lorentz contracted along $\hat{\mathbf{y}}$, hence the number density of electrons will increase as,

$$n'_e = \frac{n'_e}{\cos \theta}, \quad (3.9)$$

leading to the perhaps unexpected

$$\bar{n}'_e = \frac{\bar{n}_e}{\cos^3 \theta}. \quad (3.10)$$

Time is dilated

$$t' = \frac{t}{\cos \theta}. \quad (3.11)$$

Consider now the more general case (I should just simply replace my diagram with a 3D one that incorporates this initially) where the photon's electric field is rotated out of the x - y plane, *i.e.*

$$\mathbf{E} = E_0(-\cos \phi \sin \theta, \cos \phi \cos \theta, \sin \phi) \quad (3.12)$$

and correspondingly

$$\mathbf{B} = \frac{\hat{\mathbf{k}} \times \mathbf{E}}{c} = \frac{E_0}{c}(\sin \phi \sin \theta, -\sin \phi \cos \theta, \cos \phi). \quad (3.13)$$

The Lorentz transformations for electro-magnetic fields are

$$\mathbf{E}'_{\parallel} = \mathbf{E}_{\parallel}, \quad (3.14)$$

$$\mathbf{B}'_{\parallel} = \mathbf{B}_{\parallel}, \quad (3.15)$$

$$\mathbf{E}'_{\perp} = \gamma_{\mathbf{v}}(\mathbf{E}_{\perp} + \mathbf{v} \times \mathbf{B}), \quad (3.16)$$

$$\mathbf{B}'_{\perp} = \gamma_{\mathbf{v}}(\mathbf{B}_{\perp} - \mathbf{v} \times \mathbf{E}/c^2). \quad (3.17)$$

Using the above expressions for \mathbf{E}_{\perp} and \mathbf{E}_{\parallel} and transforming to the boosted frame,

$$\mathbf{E}' = E_0 \cos \theta(0, \cos \phi, \sin \phi). \quad (3.18)$$

As anticipated for normal incidence there is no component of the E-field normal to the surface. Conveniently, the polarisation of the incident photon is unchanged despite having components both parallel and perpendicular to the transformation and

$$|\mathbf{E}'| = |\mathbf{E}| \cos \theta. \quad (3.19)$$

The picture can now be completed. Since

$$a'_0 = \frac{e|\mathbf{E}'|}{m_e e \omega'} \quad (3.20)$$

it follows that

$$a'_0 = a_0, \quad (3.21)$$

$$S' = \frac{S}{\cos^3 \theta}. \quad (3.22)$$

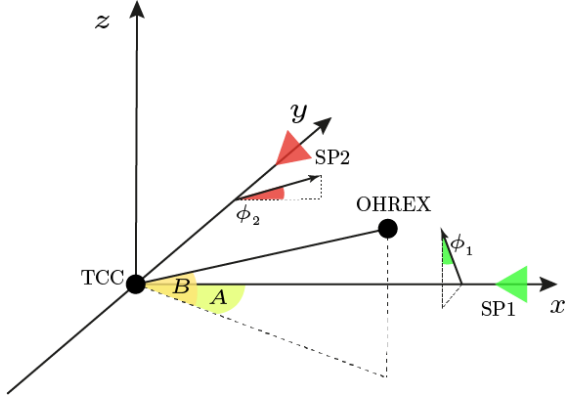


Figure 3.2: ORION target chamber geometry showing the location of the target (TCC) and OHREX spectrometer and the green (SP1) and infra-red (SP2) beamlines and their corresponding polarisations.

3.1.2 ORION interaction geometry

The ORION target chamber has its own defined geometry with the target located at the origin, described in figure 3.2. The polarisation angles are $\phi_1 = 11.8^\circ$ and $\phi_2 = 16.4^\circ$. Following reflection of the infra-red beam off the plasma mirror, both the green and infra-red lasers propagate in the $-\hat{x}$ -direction towards the origin. The OHREX crystal is located at

$$\mathbf{r}_{\text{OHREX}} = r_0(\cos B \cos A, -\cos B \sin A, \sin B), \quad (3.23)$$

where $r_0 = 2.4\text{ m}$, $A = 26.82^\circ$ and $B = 18.15^\circ$, setting the rotation angle of the target. This was achieved using the ORION Multi-Target-Mounts. Alignment was performed by Ed Gumbrell and no further details will be provided here on that process.

The interaction plane is therefore defined by the vector

$$\mathbf{n} = \frac{\mathbf{r}_{\text{OHREX}}}{r_0} \times \hat{\mathbf{x}} = (0, \sin B, \cos B \sin A). \quad (3.24)$$

The cosine rule can be applied to determine the polarisation of the laser pulses in the interaction plane, for polarisation vector $\hat{\mathbf{E}}$,

$$\frac{\mathbf{n}}{|\mathbf{n}|} \cdot \hat{\mathbf{E}} = \cos \theta, \quad (3.25)$$

where θ defines the angle between the polarisation vector and the vector normal to the interaction plane. This corresponds to angles out of the interaction plane

of 42.2 or the SP1 beam (rotating anticlockwise out of the interaction plane when looking from TCC to parabola) and 19.6 or the SP2 beam (rotating clockwise out of the interaction plane when looking from TCC to parabola). Again applying the cosine rule, the angle of incidence is 16

Next up: Polarisation on OHREX interaction plane.

The same method can be applied to determine the polarisation of the OHREX crystal interaction plane. The OHREX crystals have a nominal Bragg angle of 51.3

I still need to know the exact orientation of the OHREX but assuming it is vertical, the interaction plane is defined by

$$\mathbf{n}_O = \frac{\mathbf{r}_{\text{OHREX}}}{r_0} \times \hat{\mathbf{z}} = (-\sin A, -\cos A, 0), \quad (3.26)$$

once it has been normalised.

Then again applying the cosine rule, this plane corresponds to angles out of the interaction plane of 10.5° for SP1 and 58.9° for SP2.

Is has been assumed that the non-linear RPM mechanism retains the polarisation of the incident laser pulse in the reflected harmonic beam.

Then since the OHREX crystal reflection is a linear process, we can decompose our incident beam into its polarisation constituents and consider what their combined intensity post reflection at the detector plane will be.

Also discuss the fabulous result that generally one can simply extract the results in the Smilei units and multiply by the relevant factors of the frame of interest and thus not worry too much about frame transformations.

Also check the boosted frame results against the bouchard thesis.

Once I have finished this section I must redo boosted section since I have made a mistake there and rethink a bit about optimum theta.

I must also at some point just state that a hat indicates a normalised vector.

3.1.3 Condition on validity of hole boring expression

Robinson *et al* [robinsonHoleboringRadiationPressure2009] consider for what case is the expression they derive for hole boring valid. The case they are interested

in is what happens if the energy available for an ion to gain from crossing the pseudo-capacitor is less than the kinetic energy associated with the hole boring velocity. Their analysis applies for non-relativistic hole boring velocities and circular polarised laser pulses. This theory is now updated for the ZVP mechanism (linear polarised and relativistic ion velocities).

The so-called ‘piston’ which leads to ion hole boring is the pseudocapacitor field. In section 2.1.1, the development of that field is discussed quantitatively. The peak electric field is

$$E_C = E_L = \sqrt{\frac{I}{\epsilon_0 c}} \quad (3.27)$$

and the peak displacement of electrons is

$$\Delta x = \frac{\epsilon_0 E_C}{e n_e}. \quad (3.28)$$

Considering instead the relativistic kinetic energy gained by an ion were it to fully cross the pseudocapacitor, following equation 2.32,

$$T_i = Z_i \times \frac{1}{2} m_e c^2 \frac{a_0^2}{n_e} = \frac{IZ_i}{2cn_m a \theta r me}. \quad (3.29)$$

(The equation above needs more thinking about)

Ions are reflected provided,

$$T_i > \frac{1}{2} m_i v_{HB}^2. \quad (3.30)$$

Hmm ok so in Vincenti, they approximate electron mass as much less than ion mass and therefore neglect in the momentum calculation. It also looks like they have not done full relativistic calculation, so I cannot yet say I have that. But carrying on the derivation using Vincenti expression for simplicity:

The hole-boring velocity as calculated by Vincenti *et al* [**vincentiOpticalPropertiesRelativis**tic] is

$$\frac{v_{HB}}{c} = \sqrt{\frac{R \cos \theta}{2}} \quad (3.31)$$

So come back to this section, once I have fully written out the hole boring calcualtino in full, include also the multiple ion species stuff and this condition.

The upshot of this condition is something like: require no low charge to mass ratio ions (ie v heavy ions) and fully ionisation, these conditions are satisfied in this area of study.

To arrive at that result, useful parts include: composite mass density $\rho = \sum_i m_i n_i$, $m_i = A_i / N_A$ and $A_i \approx 2Z_i$ for most low mass ions relevant in these plasmas.

Appendices

Cor animalium, fundamentum est vitæ, princeps omnium, Microcosmi Sol, a quo omnis vegetatio dependet, vigor omnis & robur emanat.

The heart of animals is the foundation of their life, the sovereign of everything within them, the sun of their microcosm, that upon which all growth depends, from which all power proceeds.

— William Harvey [harvey_exercitatio_1628]



General plasma physics

Contents

A.1 Geometric transverse emittance	47
--	----

A.1 Geometric transverse emittance

A beam¹ of particles is fully described by its six-dimensional particle phase space distribution

$$\rho(\mathbf{x}, \mathbf{p}) = \rho(x, p_x, y, p_y, z, p_z), \quad (\text{A.1})$$

where $\mathbf{p} = p_x \hat{\mathbf{x}} + p_y \hat{\mathbf{y}} + p_z \hat{\mathbf{z}}$ is the canonical momentum [**McDonald Methods of emittance measurement 1989**]. Under the Hamilton formalism, for ideal conditions, the six-dimensional volume of the beam in this space, termed the *emittance*, arises as a conserved quantity and is therefore a useful quantity to describe the beam quality. (something to do with it affecting the ability to focus the beam?? check the papers) It is useful to rotate the coordinate system so as to align with the beam's propagation. The distribution can be written as

$$\rho(\mathbf{x}', \mathbf{p}') = \rho(x_L, p_L, x_T, p_T, x_{T'}, p_{T'}), \quad (\text{A.2})$$

¹In this section it is electron beams and not bunches that are referred to to demonstrate the generality of these concepts.

where L is longitudinal to the beam's propagation direction, and T and T' are two orthogonal directions transverse to the beam's propagation. Where discussed in this thesis, T' will unanimously refer to the z -direction, that is, the additional direction in 3D simulations, all such simulations are designed such that the z -direction is transverse to the beam propagation direction.

Recording a six-dimensional phase space in experiment is impossible while in simulations it is almost prohibitively costly in terms of data storage. Hence, it is common practice to project the distribution onto three orthogonal sub-spaces corresponding to each spatial axis, L, T and T' and compute the area on each. Note that since the electron beam is ultra-relativistic, all electrons propagate at approximately c and therefore it is the transverse and not the longitudinal emittance that describes the beam's quality. As a particle beam does not typically exist with well-defined borders, the area used to describe the emittance is restricted to an ellipse containing only the high-density core of the distribution. For a subspace i , where $i = T$ or T' , Floettmann *et al* [**floettmannBasicFeaturesBeam2003**] derive the *transverse normalised emittance* as

$$\epsilon_{n,rms}^i = \frac{1}{m_e c} \sqrt{\langle x_i^2 \rangle \langle p_i^2 \rangle - \langle x_i p_i \rangle^2}, \quad (\text{A.3})$$

where $\langle \rangle$ is the second central moment of the particle distribution,

$$\langle ab \rangle = \frac{\int ab \rho(\mathbf{x}', \mathbf{p}') dV}{\int \rho(\mathbf{x}', \mathbf{p}') dV} - \frac{\int a \rho(\mathbf{x}', \mathbf{p}') dV \int b \rho(\mathbf{x}', \mathbf{p}') dV}{(\int \rho(\mathbf{x}', \mathbf{p}') dV)^2}, \quad (\text{A.4})$$

here $dV = \Pi_j dx_j dp_j$ for $j = L, T, T'$.

When working with emittances, most frequently in the literature it is the *transverse geometric emittance*, ϵ_{rms}^i that is discussed. This is a natural consequence of it being more readily accessible in experiments [**McDonald Methods of emittance measurement 1989**]. The geometric and normalised emittances are related via

$$\epsilon_{rms}^i = \frac{\epsilon_{rms}^i}{\gamma \beta_L}, \quad (\text{A.5})$$

where $\gamma = 1/\sqrt{1-\beta^2}$ refers to the beam's mean energy and $\beta_L \approx c$ is the ultrarelativistic beam's longitudinal speed.

The Courant-Snyder invariant which describes the ellipse that corresponds to the emittance is²

$$\epsilon_{\text{rms}}^i = \gamma x_i^2 + 2\alpha x x' \beta x_i'^2, \quad (\text{A.6})$$

here the coordinates are x_i and $x'_i = p_i/p_L$ [3]. The Twiss parameters are

$$\alpha = -\frac{\langle x_i x'_i \rangle}{\epsilon_{\text{rms}}^i}, \quad (\text{A.7})$$

$$\beta = \frac{\langle x_i \rangle}{\epsilon_{\text{rms}}^i} \quad (\text{A.8})$$

and

$$\gamma = \frac{\langle x_i'^2 \rangle}{\epsilon_{\text{rms}}^i}. \quad (\text{A.9})$$

Thus the shape of the ellipse and the divergence of the beam can be determined.

²Regrettably β and γ are the standard notations for the Twiss parameters, at all other locations in this thesis, these parameters will refer to the standard relativistic beta and gamma factors of objects respectively.

The first kind of intellectual and artistic personality belongs to the hedgehogs, the second to the foxes ...

— Sir Isaiah Berlin [**berlin_hedgehog_2013**]

References

- [1] K. Miyauchi et al. “Laser Electron Acceleration by a Plasma Separator”. In: *Physics of Plasmas* 11.10 (Oct. 2004), pp. 4878–4881. (Visited on 08/31/2023).
- [2] Alex F. Savin et al. “Energy Absorption in the Laser-QED Regime”. In: *Scientific Reports* 9.1 (Dec. 2019). arXiv: 1901.08017.
- [3] wiedemann. *Particle Accelerator Physics*. New York, NY: Springer Berlin Heidelberg, 2015.